AMERICAN SOCIETY FOR MICROBIOLOGY | Journal of Bacteriology

Circuitry Linking the Catabolite Repression and Csr Global Regulatory Systems of *Escherichia coli*

Archana Pannuri,[a] Christopher A. Vakulskas,[a]* Tesfalem Zere,[a]* Louise C. McGibbon,[b] Adrianne N. Edwards,[c] Dimitris Georgellis,[d] Paul Babitzke,[b] Tony Romeo[a]

Department of Microbiology and Cell Science, University of Florida, Institute of Food and Agricultural Sciences, Gainesville, Florida, USA[a]; Department of Biochemistry and Molecular Biology, Center for RNA Molecular Biology, Pennsylvania State University, University Park, Pennsylvania, USA[b]; Department of Microbiology and Immunology, Emory University School of Medicine, Atlanta, Georgia, USA[c]; Departamento de Genética Molecular, Instituto de Fisiología Celular, Universidad Nacional Autónoma de México, Mexico City, Mexico[d]

ABSTRACT

Cyclic AMP (cAMP) and the cAMP receptor protein (cAMP-CRP) and CsrA are the principal regulators of the catabolite repression and carbon storage global regulatory systems, respectively. cAMP-CRP controls the transcription of genes for carbohydrate metabolism and other processes in response to carbon nutritional status, while CsrA binds to diverse mRNAs and regulates translation, RNA stability, and/or transcription elongation. CsrA also binds to the regulatory small RNAs (sRNAs) CsrB and CsrC, which antagonize its activity. The BarA-UvrY two-component signal transduction system (TCS) directly activates *csrB* and *csrC* (*csrB/C*) transcription, while CsrA does so indirectly. We show that cAMP-CRP inhibits *csrB/C* transcription without negatively regulating phosphorylated UvrY (P-UvrY) or CsrA levels. A *crp* deletion caused an elevation in CsrB/C levels in the stationary phase of growth and increased the expression of *csrB-lacZ* and *csrC-lacZ* transcriptional fusions, although modest stimulation of CsrB/C turnover by the *crp* deletion partially masked the former effects. DNase I footprinting and other studies demonstrated that cAMP-CRP bound specifically to three sites located upstream from the *csrC* promoter, two of which overlapped the P-UvrY binding site. These two proteins competed for binding at the overlapping sites. *In vitro* transcription-translation experiments confirmed direct repression of *csrC-lacZ* expression by cAMP-CRP. In contrast, cAMP-CRP effects on *csrB* transcription may be mediated indirectly, as it bound nonspecifically to *csrB* DNA. In the reciprocal direction, CsrA bound to *crp* mRNA with high affinity and specificity and yet exhibited only modest, conditional effects on expression. Our findings are incorporated into an emerging model for the response of Csr circuitry to carbon nutritional status.

IMPORTANCE

Csr (Rsm) noncoding small RNAs (sRNAs) CsrB and CsrC of *Escherichia coli* use molecular mimicry to sequester the RNA binding protein CsrA (RsmA) away from lower-affinity mRNA targets, thus eliciting major shifts in the bacterial lifestyle. CsrB/C transcription and turnover are activated by carbon metabolism products (e.g., formate and acetate) and by a preferred carbon source (glucose), respectively. We show that cAMP-CRP, a mediator of classical catabolite repression, inhibits *csrC* transcription by binding to the upstream region of this gene and also inhibits *csrB* transcription, apparently indirectly. We propose that glucose availability activates pathways for both synthesis and turnover of CsrB/C, thus shaping the dynamics of global signaling in response to the nutritional environment by poising CsrB/C sRNA levels for rapid response.

The Csr (carbon storage regulator) or Rsm (repressor of stationary-phase metabolites) system is a widely conserved bacterial posttranscriptional regulatory system (1–3). Its components, their functions, and the mechanisms by which the central regulator of this system, CsrA or RsmA, affects gene expression have been studied primarily in *Gammaproteobacteria* (4–6). The sequence-specific RNA binding protein CsrA regulates translation, stability, and/or transcription or elongation of numerous target mRNAs. CsrA regulates the expression of genes involved in lifestyle transitions. In *Escherichia coli*, CsrA activates glycolysis and central carbon pathways (7–13) and motility (14, 15). Conversely, it represses gluconeogenesis (7), glycogen biosynthesis (16–20), biofilm formation (21–24), the stringent response (25), and expression of genes involved in other stress resistance and stationary-phase processes, e.g., *cstA*, *hfq*, *cel*, *sdiA*, and *nhaR* (24, 26–30). Its effects on pathogenesis are complex. For example, CsrA both positively and negatively affects expression of enteropathogenic *E. coli* (EPEC) pathogenicity island genes (31, 32). CsrA was found to copurify with over 700 different mRNAs in *E. coli* K-12 (25) and to affect the expression of hundreds of genes (33).

Consistent with its extensive regulatory role, CsrA activity is tightly controlled. In *E. coli*, *csrA* is transcribed from five promot-

Received 7 June 2016 **Accepted** 12 August 2016

Accepted manuscript posted online 22 August 2016

Citation Pannuri A, Vakulskas CA, Zere T, McGibbon LC, Edwards AN, Georgellis D, Babitzke P, Romeo T. 2016. Circuitry linking the catabolite repression and Csr global regulatory systems of *Escherichia coli*. J Bacteriol 198:3000–3015. doi:10.1128/JB.00454-16.

Editor: R. L. Gourse, University of Wisconsin—Madison

Address correspondence to Tony Romeo, tromeo@ufl.edu.

* Present address: Christopher A. Vakulskas, Integrated DNA Technologies, Molecular Genetics Department, Coralville, Iowa, USA; Tesfalem Zere, Department of Oral Biology, College of Dentistry, University of Florida, Gainesville, Florida, USA.

ers using two different sigma factors (34). Furthermore, CsrA directly represses its own translation while indirectly activating its transcription (34). CsrA activity is antagonized by the noncoding small RNAs (sRNAs) CsrB and CsrC, which contain multiple CsrA binding sites that allow them to sequester this protein (35, 36). Fluctuations in the levels of these RNAs regulate CsrA activity in response to the environment. Transcription of both *csrB* and *csrC* (*csrB/C*) is activated by the BarA-UvrY two-component signal transduction system (TCS) in response to carboxylic acids such as formate and acetate (3, 36–41). CsrA indirectly activates transcription of CsrB and CsrC through its effects on BarA-UvrY, creating a negative-feedback loop within the Csr circuitry (37, 38, 42). CsrB/C turnover requires the GGDEF-EAL domain protein CsrD, which is necessary for cleavage by RNase E and turnover (42, 43). Therefore, CsrD affects the expression of CsrA-regulated genes and processes. Recent studies showed that glucose availability activates CsrB/C decay. The unphosphorylated form of $EIIA^{Glc}$ of the phosphoenolpyruvate:carbohydrate phosphotransferase system (PTS), which predominates during glucose transport, binds to the EAL domain of CsrD (44). We previously proposed a model for the influence of carbon nutrition on the workings of the Csr system based on these observations. The elimination of a preferred carbon source and the buildup of carboxylic acid products of metabolism together facilitate CsrB/C sRNA accumulation, inhibit CsrA activity, and promote the physiological switch from the exponential phase to the stationary phase of growth and a stress-resistant phenotype (43, 44).

Noteworthy among the many *E. coli* mRNAs that copurified with CsrA were transcripts for global regulatory factors such as *relA* and *dksA* of the stringent response system and *crp* and *cyaA* of the catabolite repression system (25). Reciprocal regulatory interactions between the Csr and stringent response systems permit the Csr system to posttranscriptionally reinforce the transcriptional effects of DksA and (p)ppGpp on the expression of genes that are coregulated by these systems (25). Details of the interactions between the Csr and catabolite repression regulatory systems were not previously determined and are the subject of the present study.

The genes *crp* and *cyaA* encode the cyclic AMP (cAMP) receptor protein (CRP) and the enzyme that synthesizes cAMP, adenylate cyclase, respectively. The cAMP-CRP complex regulates transcription in response to the availability of a preferred carbon source, e.g., glucose (45–47). Under conditions of carbon limitation, the PTS proteins, including the glucose-specific protein $EIIA^{Glc}$, are predominantly phosphorylated. In this form, P-$EIIA^{Glc}$ binds to adenylate cyclase and activates cAMP synthesis (48). Transport and phosphorylation of glucose or other PTS sugars leads to dephosphorylation of $EIIA^{Glc}$ and loss of its ability to activate cAMP synthesis. The cAMP-CRP complex mediates hierarchical utilization of nonpreferred carbon sources, referred to as carbon catabolite repression (CCR), by activating the expression of genes required for the transport and utilization of alternative carbon sources (49). cAMP-CRP also influences the expression of genes not directly involved in carbon metabolism such as those encoding ribosomal proteins, tRNAs, amino acid biosynthesis enzymes, heat shock proteins, sRNAs, and perhaps as many as 70 transcription factors (45–47, 50–55). cAMP levels and cAMP-CRP regulatory functions have been suggested to respond to both the carbon status and the nitrogen status of the cell, leading to reorganization of the proteome (56).

cAMP-CRP is a bifunctional protein that can activate or repress transcription (57). As a transcriptional activator, cAMP-CRP binds to a sequence located upstream from (class I activation) or close to (class II activation) promoter DNA and participates in protein-protein interactions leading to transcription initiation by RNA polymerase (58). Activation using CRP binding sites positioned farther upstream from the promoter requires cAMP-CRP to work in conjunction with other regulatory proteins and may involve protein-protein interactions and/or DNA bending. DNA binding mechanisms similar to those observed in activation are employed when cAMP-CRP acts as a repressor (57).

Bioinformatics analysis for potential cAMP-CRP binding sites in the *E. coli* genome identified the coding region of *syd*, the gene immediately upstream from *csrB*, as a possible target (47). In addition, an online tool (Virtual Footprint [www.prodoric.de/vfp]) for predicting the binding sequences of regulatory proteins identified potential CRP binding sites in *csrB*, *csrC*, *csrA*, *csrD*, and *uvrY*. Also, possible reciprocal regulatory interactions between cAMP-CRP and the Csr system prompted us to undertake the present study. We provide evidence that cAMP-CRP inhibits the transcription of *csrC* directly and that of *csrB* indirectly, while CsrA modestly and conditionally activates *crp* expression. The implications of this new circuitry for determining the complex global regulatory response of *E. coli* to its carbon nutritional environment are discussed.

MATERIALS AND METHODS

Bacterial strains and growth conditions. The strains, plasmids, and bacteriophage used in this study are listed in Table 1. Oligonucleotides are listed in Table 2. Unless otherwise indicated, bacteria were grown at 37°C, with shaking at 250 rpm, in Luria-Bertani (LB) medium (59), LB medium buffered with 0.1 M MOPS (3-morpholinopropane-1-sulfonic acid) (LB-MOPS) and with or without an added carbon source, or Kornberg (KB) medium (1.1% K_2HPO_4, 0.85% KH_2PO_4, 0.6% yeast extract containing 0.5% glucose for liquid medium). Media were supplemented with antibiotics at the following concentrations or as indicated otherwise: kanamycin at 100 μg/ml; ampicillin at 100 μg/ml; chloramphenicol at 25 μg/ml, and tetracycline at 10 μg/ml. P1*vir* transductions were performed as previously described (59).

Construction of *lacZ* reporter fusions. Single-copy, chromosomally integrated transcriptional and translational fusions to *lacZ* were constructed using the CRIM system (60) with plasmid vectors pLFX and pLFT, derived from pAH125 (25), and integrated into the chromosome at the λ *att* site, and single integrants were confirmed by PCR, as described previously (60).

For constructing *csrB-lacZ and csrC-lacZ* transcriptional fusions, 502 (−500 to +2 with respect to the *csrB* transcription initiation site)-nucleotide (nt) and 304 (−301 to +3 with respect to the *csrC* transcription initiation site)-nt regions of *csrB* and *csrC* were amplified by PCR from *E. coli* MG1655 genomic DNA using primer pairs csrB lacZ Fwd/csrB lacZ Rev and csrC lacZ Fwd/csrC lacZ Rev. PCR products were gel purified, digested with PstI and KpnI, ligated to PstI- and KpnI-digested and dephosphorylated plasmid pLFX, and electroporated into DH5αλpir cells. Sequence-verified plasmids pLFXcsrB-lacZ and pLFXcsrC-lacZ were integrated into the λ *att* site of *E. coli* MG1655 Δ*lacZ*, using helper plasmid pPFINT.

For constructing the *crp′-′lacZ* translational fusion, the primer pair crp trsln Fwd/crp trsln Rev was used to amplify a 677-nucleotide region (nucleotides −667 to +10 with respect to the translational start site) of *crp* from MG1655. The resulting PCR product was gel purified, digested with PstI and EcoRI, ligated to PstI- and EcoRI-digested, dephosphorylated plasmid pLFT, and electroporated into DH5αλpir cells. Primer pair cyaA

TABLE 1 List of the strains, plasmids, and bacteriophage used in this study[a]

Strain, plasmid, or bacteriophage	Genotype or description	Source or reference
E. coli strains		
MG1655	F$^-$ λ$^-$ *rph-1*	CGSC (no. 6300)
AP379	MG1655 Δ*lacZ*	This study
AP455	MG1655 *crp*::*cam*	This study
AP1000	MG1655 *cyaA*::*kan*	This study
AP779	MG1655 Δ*csrD*::*kan*	This study
AP792	MG1655 Δ*csrD*::*kan crp*::*cam*	This study
AP461	MG1655 Δ*lacZ*/pLFXcsrB-*lacZ*	This study
AP482	MG1655 Δ*lacZ*/pLFXcsrB-*lacZ crp*::*cam*	This study
AP858	MG1655 Δ*lacZ*/pLFXcsrC-*lacZ*	This study
AP864	MG1655 Δ*lacZ*/pLFXcsrC-*lacZ crp*::*cam*	This study
AP724	MG1655 Δ*lacZ*/pLFTcrp′-′*lacZ*	This study
AP736	MG1655 Δ*lacZ*/pLFTcrp′-′*lacZ csrA*::*kan*	This study
AP804	MG1655 uvrY::3× FLAG	This study
AP854	MG1655 uvrY::3× FLAG *crp*::*cam*	This study
CF7789	MG1655 Δ*lacI-Z* (MluI)	Michael Cashel
PLB2286	CF7789 *crp′-′lacZ*	This study
PLB2287	CF7789 *crp′-′lacZ csrA*::*kan*	This study
PLB2289	CF7789 *cyaA′-′lacZ*	This study
PLB2290	CF7789 *cyaA′-′lacZ csrA*::*kan*	This study
BL21(λDE3)	F$^-$ *lon-11* Δ(*ompT-nfrA*)*885* Δ(*galM-ybhJ*)*884* λDE3 [*lacI lacUV5*-T7 gene 1 *ind1 sam7 nin5*] Δ*46* [*mal*$^+$]$_{K\text{-}12}$ (λ^s) *hsdS10*	Novagen
Plasmids		
pLFX	Plasmid used for constructing transcriptional fusions	25
pLFT	Plasmid used for constructing translational fusions	25
pPFINT	Helper plasmid used for integrating *lacZ* fusions into the chromosome	25
pET24a	Plasmid used for constructing *crp* clone for expressing the CRP protein	Novagen
pLFXcsrC-lacZ	*csrC* upstream region cloned into pLFX	This study
Bacteriophage P1*vir*	Strictly lytic P1	Carol Gross

[a] Strains harboring *crp*::*cam*, *cyaA*::*kan*, *csrD*::*kan*, and *csrA*::*kan* mutations were obtained by P1*vir* transduction. CGSC, *E. coli* Genetic Stock Center.

trsln Fwd/cyaA trsln Rev was used to amplify a 497-nucleotide region (nucleotides −438 to +59 with respect to the *cyaA* translational start site) of *cyaA* from MG1655, gel purified, digested with PstI and BamHI, ligated to PstI- and BamHI-digested, dephosphorylated plasmid pLFT, and electroporated into DH5αλpir cells. The sequence-verified plasmids, pLFTcrp′-′lacZ and pLFTcyaA′-′lacZ, were integrated into the λ *att* site of *E. coli* MG1655 Δ*lacZ* using helper plasmid pPFINT.

β-Galactosidase and protein assays. Assays to examine the effects of *csrA* on expression of *cyaA′-′lacZ* and *crp′-′lacZ* translational fusions were performed as described previously (19). Assays to examine the effects of cAMP-CRP on *csrB-lacZ* and *csrC-lacZ* transcriptional fusions were conducted as described previously (61) with minor modifications (25). Total cell protein was measured after precipitation with 10% trichloroacetic acid, using the bicinchoninic acid assay (Pierce Biotechnology) with bovine serum albumin as a protein standard. Purified proteins were quantified similarly but without trichloroacetic acid precipitation.

Northern blotting. Total RNA was isolated using a RiboPure-Bacteria kit (Ambion) or by phenol-chloroform extraction. Phenol-chloroform extraction was performed following the Gross Lab protocol (http://derisilab.ucsf.edu/microarray/pdfs/Total_RNA_from_Ecoli.pdf) for isolation of total RNA from *E. coli*. For Northern blotting, 2 μg of total RNA was mixed with 2 volumes of loading buffer (50% [vol/vol] deionized formamide; 6% [vol/vol] formaldehyde; 1× MOPS [20 mM]; 5 mM sodium acetate [NaOAc]; 2 mM EDTA [pH 7.0]; 10% [vol/vol] glycerol; 0.05% [wt/vol] bromophenol blue; 0.01% [wt/vol] ethidium bromide), denatured by heating at 75°C for 5 min, chilled on ice, and separated by electrophoresis on a 7 M urea–5% polyacrylamide gel. RNA was transferred overnight to a positively charged nylon membrane (Roche) in 1× Tris-borate-EDTA (TBE) buffer and fixed to the membrane by UV cross-linking. The rRNA that was transferred was stained with methylene blue and imaged using a Gel-Doc, and its signal intensity was quantified using Quantity One software. CsrB or CsrC RNAs were detected with DIG-labeled RNA probes according to a digoxigenin (DIG) Northern starter kit manual (Roche), and the signals were captured with a Chemi-Doc XRS+ system (Bio-Rad, Hercules, CA).

Construction of a carboxy-terminal FLAG-tagged UvrY protein. A strain expressing a recombinant UvrY protein containing a 3× FLAG tag at the carboxy terminus from the native *uvrY* locus was constructed as described earlier (62). The recombinant UvrY$_{FLAG}$ protein appeared to be fully functional, as determined by its ability to activate the synthesis of CsrB and CsrC RNAs relative to the results seen with the wild-type (WT) UvrY protein (data not shown).

Western blotting of CsrA and UvrY-FLAG. For Western blotting, cultures were grown with shaking at 37°C at 250 rpm and harvested throughout the growth curve. Cells were mixed with 2× sample buffer (4% [wt/vol] SDS; 0.16 M Tris; 1.5% [vol/vol] β-mercaptoethanol; 20% [vol/vol] glycerol; 0.02% [wt/vol] bromophenol blue, pH 6.0) and lysed by sonication and then by boiling. Samples (1 to 5 μg of total cellular protein) were subjected to SDS-PAGE, transferred to 0.2 μM polyvinylidene difluoride (PVDF) membranes, and detected using polyclonal anti-CsrA, monoclonal anti-FLAG (for UvrY-FLAG), or anti-RpoB (for RpoB) antibodies as described previously (62). Unphosphorylated UvrY was resolved from phosphorylated UvrY (P-UvrY) on SDS gels containing Phos-Tag reagent, as described previously (62).

TABLE 2 List of oligonucleotides used in this study

Oligonucleotide	Sequence	Purpose
csrB lacZ Fwd	5′-GTCCTGCAGCCGGGGATATGCACGCGCAGTTTGT-3′	Forward primer for constructing *csrB-lacZ* transcriptional fusion
csrB lacZ Rev	5′-GTCGGTACCACGAAGATAGAATCGTCTTTTTCG-3′	Reverse primer for constructing *csrB-lacZ* transcriptional fusion
csrC lacZ Fwd	5′-GTCCTGCAGAATGCGTCTGTTGATAATTCAAATTAGTC-3′	Forward primer for constructing *csrC-lacZ* transcriptional fusion
csrC lacZ Rev	5′-GTCGGTACCTATGGGTGCTACTTTACGCCTTTGC-3′	Reverse primer for constructing *csrC-lacZ* transcriptional fusion
crp trsln Fwd	5′-GCATGACTGCAGCGCTTTTTCCAGCATCAACGCCACTG-3′	Forward primer for constructing *crp′-′lacZ* translational fusion
crp trsln Rev	5′-GTCGTCGAATTCCAAGCATGCGCGGTTATCCTCTG-3′	Reverse primer for constructing *crp′-′lacZ* translational fusion
cyaA trsln Fwd	5′-TATACTGCAGAGAGTGCAAGTGGGCTTTG-3′	Forward primer for constructing *cyaA′-′lacZ* translational fusion
cyaA trsln Rev	5′-TATAGGATCCACACGCAATTGATTTATGGC-3′	Reverse primer for constructing *cyaA′-′lacZ* translational fusion
crp WT Fwd SP6	5′-ATTTAGGTGACACTATAGAAGATGCTACAGTAATACATTGATGTAC TGCATGTATGC-3′	Forward primer for generating template for *crp* WT RNA
crp P1 Rev	5′-CCAAGCACCATGCGCGGTTATCCTCTG-3′	Reverse primer for generating *crp* template for WT RNA
cyaA WT Fwd T7	5′-TAATACGACTCACTATAGGGTTTTAGACCATTT-3′	Forward primer for generating template for *cyaA* WT RNA
cyaA WT Rev T7	5′-TTTATGGCATCCAGTCTCTGT-3′	Reverse primer for generating template for *cyaA* WT RNA
crp Fwd Exp	5′-GTCGTCGGATCCATGGTGCTTGGCAAACCGCAAACAG-3′	Forward primer for cloning *crp* coding region into pET24a vector
crp Rev Exp	5′-GTAGTACTCGAGTTAACGAGTGCCGTAAACGACGATG-3′	Reverse primer for cloning *crp* coding region into pET24a vector
UvrY-His-F	5′-TAGCTACTACTCGAGCTGACTTGATAATGTCTCCGCATTACA CAG-3′	Forward primer for cloning *uvrY* coding region into pET24a vector
UvrY-His-R	5′-CGAGTTCTTCATATGATCAACGTTCTACTTGTTGATGACCACGAA-3′	Reverse primer for cloning *uvrY* coding region into pET24a vector
csrB DBA Fwd	5′-TCTGGTGACTCAGAAAAGGCTAAAACTGCCG-3′	Forward primer for generating *csrB* DNA for binding assays
csrB DBA Rev	5′-GAAGATAGAATCGTCTTTTTCGCGAAGTCTTACAAGG-3′	Reverse primer for generating *csrB* DNA for binding assays
csrC DBA Fwd	5′-GCGTGAGCGTTGTAAGTAAAAGCCATACGC-3′	Forward primer for generating *csrC* DNA for binding assays
csrC DBA Rev	5′-GGGTGCTACTTTACGCCTTTGCTTTAAACAAACAATCAACC-3′	Reverse primer for generating *csrC* DNA for binding assays
csrB DFP Fwd	5′-CAGGAAAATCTGATTGGTCATCTGGTGAC-3′	Forward primer for generating *csrB* template for footprinting
csrB DFP Rev	5′-GTGTCATCATCCTGATGTTCACTTCGTTG-3′	Reverse primer for generating *csrB* template for footprinting
csrC DFP Fwd	5′-CAGGCGCACTCATCACAAAATGCGTCTG-3′	Forward primer for generating *csrC* template for footprinting
csrC DFP Rev	5′-GTCTCCGGACGTTTGTCTTCCTGAC-3′	Reverse primer for generating *csrC* template for footprinting
csrB (*Ec*) probe Rev T7	5′-TAATACGACTCACTATAGGGTTCGTTTCGCAGCATTCCAG-3′	Reverse primer for generating T7 template for CsrB riboprobe in *E. coli*
csrB (*Ec*) probe Fwd	5′-GCGTTAAAGGACACCTCCAGG-3′	Forward primer for generating T7 template for CsrB riboprobe in *E. coli*
csrC (*Ec*) probe Rev T7	5′-TAATACGACTCACTATAGGGTCTTACAATCCTTGCAGGC-3′	Reverse primer for generating T7 template for CsrC riboprobe in *E. coli*
csrC (*Ec*) probe Fwd	5′-GAGGACGCTAACAGGAACAATG-3′	Forward primer for generating T7 template for CsrC riboprobe in *E. coli*
uvrY 3× FLAG Fwd	5′-TCGCCATGGTCTGTGTAATGCGGAGACATTATCAAGTCAGGACTAC AAAGACCATGACGG-3′	Forward primer for constructing *uvrY*::3× FLAG
uvrY 3× FLAG Rev	5′-GTTACGGTTTTTAAAAACGCTTTTGCGTCAAACTGATCACCATATGA ATATCCTCCTTAG-3′	Reverse primer for constructing *uvrY*::3× FLAG

Electrophoretic gel mobility shift assays (EMSA) for RNA binding. Binding of CsrA to *crp* and *cyaA* transcripts was determined by EMSA with *in vitro*-synthesized *crp* and *cyaA* transcripts (MAXIscript SP6/MEGAshortscript kit; Ambion) and recombinant CsrA-His_6 (2). The template DNA for *in vitro* transcription of *crp* and *cyaA* was generated by PCR from MG1655 genomic DNA, using oligonucleotide pairs crp WT Fwd SP6/crp P1 Rev (*crp* WT) and cyaA WT Fwd T7/cyaA WT Rev T7 (*cyaA* WT). WT *crp* transcripts (178 nt, consisting of 167 nt of the noncoding mRNA leader and 11 nt of the coding region) and *cyaA* transcripts (201 nt, consisting of 154 nt of the noncoding mRNA leader and 47 nt of the coding region) were gel purified, treated with Antarctic phosphatase (NEB), and radiolabeled at the 5′ end using [γ-^{32}P]ATP and T4 polynucleotide kinase. Binding reaction mixtures contained 0.6 nM RNA, 10 mM $MgCl_2$, 100 mM KCl, 32.5 ng total yeast RNA, 20 mM dithiothreitol (DTT), 7.5% glycerol, 4 U SUPERasin (Ambion), and various concentrations of CsrA (0 to 640 nM) and were incubated at 37°C for 30 min. Reaction mixtures were separated on 9% native polyacrylamide gels using 1× TBE buffer as the electrophoresis buffer, and labeled RNA was analyzed using a phosphorimager equipped with Quantity One software, as described previously (25).

Purification of native CRP protein. The *E. coli crp* coding region was PCR amplified from MG1655 genomic DNA using the primer pair crp Fwd Exp/crp Rev Exp. The resulting PCR product was gel purified, digested with EcoRI and XhoI, ligated to EcoRI and XhoI digested, dephosphorylated pET24a(+), and transformed into DH5α cells. The resulting clone pET24a(+) *crp* was verified by sequencing and transformed into the expression host, BL21(λDE3). Shaking cultures of BL21(λDE3) pET24a(+) *crp* were grown in LB (300 ml) containing kanamycin at 37°C for 3 h, and expression of *crp* was induced for 3 h with 1 mM isopropyl-β-D-thiogalactopyranoside (IPTG). Cells were collected by centrifugation, resuspended in 30 ml of binding buffer (20 mM Tris-HCl [pH 7.9]; 500 mM NaCl; 20 mM imidazole), lysed using a French press, and centrifuged to remove cell debris from the cell lysate. The native CRP protein was fractionated using HisTrap column chromatography (63). The cell lysate was loaded onto a His-Trap column (HisTrap HP; GE Healthcare), rinsed with binding buffer (20 mM Tris-HCl [pH 7.9]; 500 mM NaCl; 20 mM imidazole), and eluted with a gradient of binding buffer and elution buffer (20 mM Tris-HCl [pH 7.9]; 500 mM NaCl; 500 mM imidazole). CRP-containing fractions were pooled and dialyzed against a buffer containing 50 mM Tris-HCl (pH 7.6], 200 mM KCl, 10 mM $MgCl_2$, 0.1 mM EDTA, 1 mM DTT, and 10% glycerol. The final CRP solution was adjusted to 50% glycerol and stored at −20°C. Purity was estimated to be ≥98% by SDS-PAGE.

Purification of carboxy-terminal His-tagged UvrY protein. His_6-tagged UvrY protein was purified from a strain expressing the recombinant protein as described previously (3).

***In vitro* phosphorylation of UvrY.** UvrY protein was phosphorylated by incubation with 100 mM lithium potassium acetyl-phosphate (Sigma-Aldrich) for 60 min at room temperature in a buffer containing 50 mM HEPES, 100 mM NaCl, and 10 mM $MgCl_2$ as described previously (40).

Electrophoretic gel mobility shift assays for DNA binding. For DNA gel shift assays, the regions from nt −400 to −1 and nt −200 to −1, with respect to the transcriptional start sites of *csrB* and *csrC*, respectively, were amplified by PCR from MG1655 genomic DNA and subjected to end labeling with [γ-^{32}P]ATP using T4 polynucleotide kinase. Binding reaction mixtures (10 μl) contained 0.5 nM end-labeled DNA, 20 mM Tris HCl (pH 7.5), 10% (vol/vol) glycerol, 50 mM KCl, 3 mM $MgCl_2$, 1 mM dithiothreitol, 100 μg/ml bovine serum albumin, and, as indicated, cAMP, CRP, and/or P-UvrY. Reaction mixtures were incubated for 30 min at 37°C degrees, and then 1 μl xylene cyanol was added and samples were separated by electrophoresis on 6% native polyacrylamide gels with 0.5× TBE buffer as the running buffer. The gels were dried, and radioactive signals were captured by phosphorimaging and analyzed using Quantity One software.

DNase I footprinting. DNA of *csrB* and *csrC* regions, extending from nt −420 to +46 and nt −319 to +100 relative to the respective transcriptional start sites, was amplified by PCR from MG1655 to generate the *csrB* and *csrC* templates for footprinting. To label the 5′ end of the nontemplate or template strand, a ^{32}P end-labeled forward or reverse primer, respectively, was used in the PCR and the resulting PCR product was gel purified. Binding reaction mixtures (10 μl) contained labeled DNA (0.5 nM), 20 mM Tris HCl (pH 7.5), 10% (vol/vol) glycerol, 50 mM KCl, 3 mM $MgCl_2$, 1 mM dithiothreitol, 100 μg/ml BSA, 200 μM cAMP, and CRP or P-UvrY. Reaction mixtures were incubated for 30 min at 37°C and cooled on ice. Then, a solution containing 0.025 U of DNase I (Roche) and $CaCl_2$ (1 mM final concentration) was added, and the contents were gently mixed by pipetting and incubated in a 37°C water bath for 1 min. Thereafter, DNase I was heat inactivated at 75°C for 10 min, samples were chilled on ice, and 2 vol of loading buffer was added. The DNA was denatured by heating at 95°C for 5 min and separated by electrophoresis on a 7 M urea–6% polyacrylamide gel. After electrophoresis, the gel was dried and radioactive signals were collected by phosphorimaging and quantified using Quantity One software. Sequencing ladders were prepared with the use of a ThermoSequenase cycle sequencing kit (Affymetrix, USB; catalog no. 78500), as recommended by the manufacturer.

***In vitro* coupled transcription-translation.** Coupled transcription-translational assays for expression of pLFXcsrC-lacZ were performed with S-30 extracts prepared from a *uvrY*-deficient strain (CF7789 *uvrY*::*cam*) as described previously (38, 61), except that the reaction mixtures were assembled to reach 32 μl and contained 0.5 U *E. coli* RNA polymerase holoenzyme and 3 μl of [^{35}S]methionine (1,175 Ci/mmol). Radiolabeled proteins were separated by electrophoresis through Bis-Tris SDS-PAGE. Gels were stained, destained, and dried, and radioactive signals were detected by phosphorimaging and quantified using Quantity One Software.

RESULTS

CRP represses *csrB* and *csrC* expression. To examine the *in vivo* effects of CRP on the expression of CsrB and CsrC RNAs, we first monitored its effects on *csrB-lacZ* and *csrC-lacZ* transcriptional fusions. While a *crp* mutant grows more slowly than the isogenic WT strain in media lacking a preferred carbon source, including LB, we found that the two strains grew equally well on LB-MOPS buffered medium containing 0.2% fructose (Fig. 1A and C). Furthermore, relative to glucose transport, fructose favors the phosphorylated form of $EIIA^{Glc}$ (P-$EIIA^{Glc}$) (64), which activates cAMP synthesis. In this medium, *csrB-lacZ* expression in isogenic WT and isogenic *crp* mutant strains increased during the exponential phase of growth and decreased as the cultures approached the stationary phase of growth (Fig. 1A). Expression of the *csrB-lacZ* fusion ranged from 2-fold to 15-fold greater in the *crp* mutant than in the WT strain in the exponential phase of growth (2 to 5 h) and decreased to similar levels in both strains thereafter. Expression of *csrC-lacZ* increased in the exponential phase up to the late exponential phase and decreased slightly thereafter in both the WT and *crp* mutant strains (Fig. 1C). Expression was ~2-fold greater in the *crp* mutant throughout the growth curve. To determine if the effect of the *crp* mutation on *csrB-lacZ* and *csrC-lacZ* expression was due to an inability to form the cAMP-CRP complex, we examined the effects of *crp* and *cyaA* mutations in the presence and absence of exogenous cAMP. The addition of cAMP was expected to restore cAMP-CRP formation in the *cyaA* mutant but not in the *crp* strain. As seen before, at 3 h (Fig. 1A), we observed that *csrB-lacZ* expression was substantially greater in the *crp* mutant as well as in the *cyaA* mutant (Fig. 1B). Addition of cAMP (10 mM) to the *cyaA* mutant culture caused a dramatic decrease in *csrB-lacZ* expression, whereas only a small decrease was observed in the *crp* mutant (Fig. 1B). The *cyaA* and *crp* mutations both caused a modest (~2-fold to 3-fold) increase in *csrC-lacZ* expression, while cAMP restored expression to normal WT levels only in the *cyaA* mutant (Fig. 1D). These results indicated that transcription of *csrB* and *csrC* is negatively influenced by cAMP-CRP.

We next determined the effect of CRP on CsrB and CsrC RNA levels in strains grown in LB-MOPS with 0.2% fructose using Northern blotting, which would reflect the effects of CRP on *csrB/C* transcription as well as on CsrB/C RNA decay. CsrB levels in the WT strain were relatively constant through the exponential phase of growth in this medium and decreased in the stationary phase (Fig. 2A). CsrC levels also decreased as the culture entered the stationary phase. While the CsrB/C RNA levels were expected to differ between the WT and the *crp* mutant in the exponential phase of growth, based on the behavior of the corresponding *lacZ* fusions (Fig. 1A and C), they were not substantially altered by the *crp* mutation. On the other hand, in the stationary phase of growth (8 and 10 h), levels of both CsrB and CsrC were elevated in the *crp*

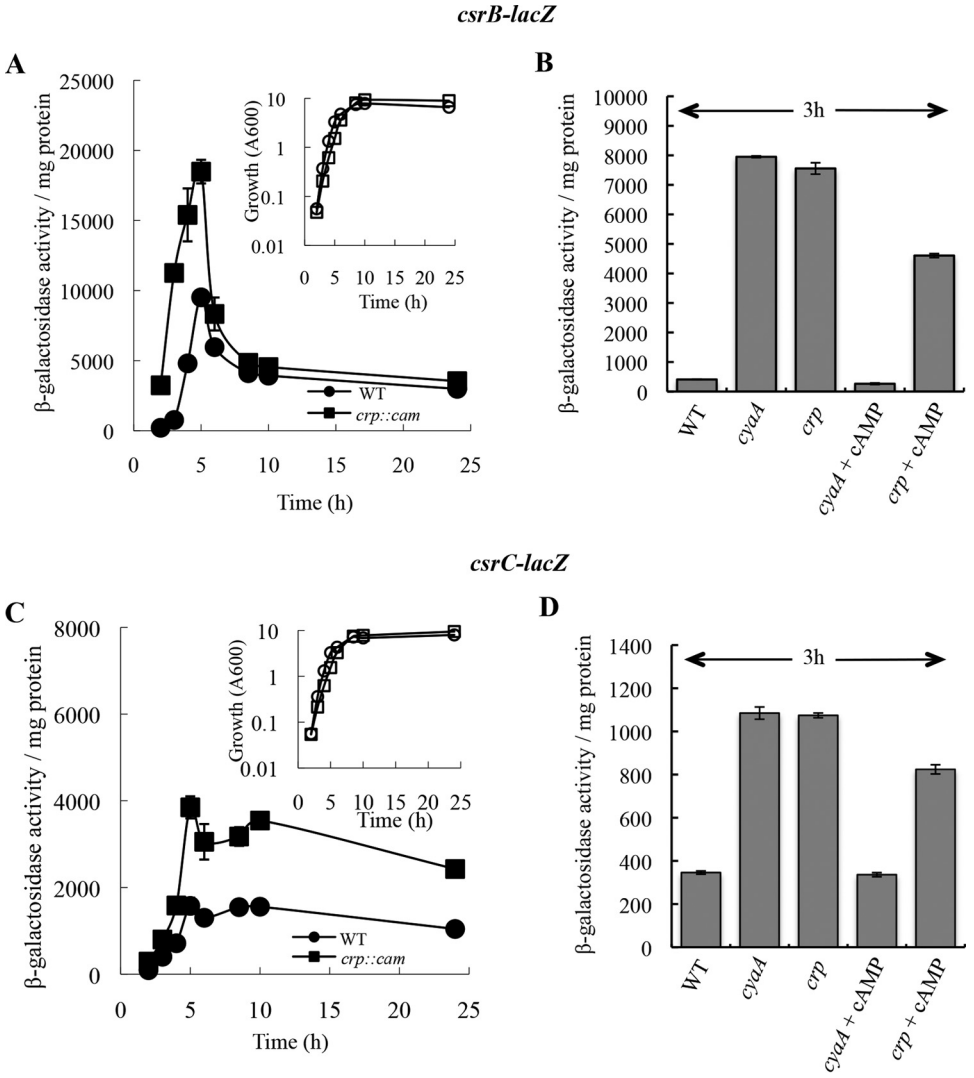

FIG 1 cAMP-CRP represses expression of *csrB-lacZ* (A and B) and *csrC-lacZ* (C and D) transcriptional fusions. *E. coli* MG1655 Δ*lacZ* (WT) and its isogenic *crp* or *cyaA* mutant, harboring chromosomal *csrB-lacZ* or *csrC-lacZ* fusions, were cultured in LB-MOPS buffered medium with 0.2% fructose, and β-galactosidase levels were determined. (A and C) Enzyme-specific activity (main panels) and growth (insets) of the WT strain and *crp* mutant. (B and D) cAMP was included in the growth medium, as indicated, at a final concentration of 10 mM. Error bars show means ± standard deviations (SD) of results of experiments that were conducted twice.

mutant, although by 24 h this difference was much less pronounced.

A possible explanation for the finding that CsrB and CsrC RNA levels were lower than expected in the *crp* mutant during exponential phase is that their decay rates may be increased in this strain. To test this idea, we determined the decay rates of CsrB and CsrC in WT (MG1655) and *crp* mutant strains in the mid-exponential phase, where *crp* disruption increased the expression of *csrB-lacZ* and *csrC-lacZ* reporter fusions (Fig. 1A and C) without substantially affecting the steady-state levels of the small RNAs (Fig. 2A). Total RNA was isolated from cells at several times following rifampin addition to block transcription, and CsrB and CsrC sRNAs were detected by Northern blotting. The half-lives of Csr small RNAs in the WT and *crp* mutant, respectively, were 2.7 and 1.3 min for CsrB and 3.9 and 1.7 min for CsrC (Fig. 2B). Thus, the decay of CsrB and CsrC was accelerated approximately 2-fold in the *crp* mutant, explaining the distinct behavior of the reporter fusions versus the steady-state levels of these RNAs in response to CRP.

Degradation of CsrB and CsrC requires the protein CsrD, which facilitates endonucleolytic cleavage of these sRNAs by RNase E (42, 43). Thus, the effect of CRP on synthesis of CsrB and CsrC under conditions of greatly reduced turnover was examined in a Δ*csrD* strain (Fig. 2C). In exponential phase (3.5 and 5 h), CsrB levels were approximately 3-fold higher in the *csrD crp* double mutant than in the *csrD* mutant background (Fig. 2C), while the effect was minimal thereafter. The CsrC levels were 2.9-, 3.6-, and 1.8-fold higher in the *csrD crp* double mutant at 5, 6.5, and 8 h of growth, respectively (Fig. 2C). Thus, in the relative absence of their decay, CsrB and CsrC RNA levels responded to CRP similarly to those seen with the *csrB-lacZ* and *csrC-lacZ* transcriptional fusions (Fig. 1). We also examined the effect of *crp* and *cyaA* mutations on CsrB and CsrC levels in LB-MOPS medium under a growth condition with minimal availability of a preferred source

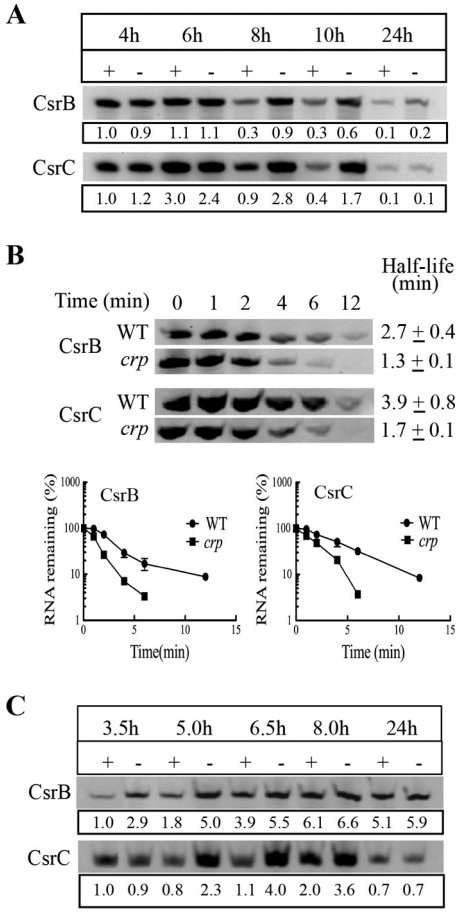

FIG 2 Effects of cAMP-CRP on CsrB and CsrC levels and decay rates. (A) Relative steady-state CsrB and CsrC levels in MG1655 (+) and its isogenic *crp* mutant (−). (B) Turnover of CsrB and CsrC sRNAs in the mid-exponential phase (3.5 h) of growth, following addition of rifampin. (C) CsrB and CsrC levels in a Δ*csrD* genetic background, which compromises their turnover. All *E. coli* strains were grown in LB-MOPS buffered medium with 0.2% fructose. For panels A and C, CsrB or CsrC levels are indicated with respect to the *crp* WT strain (+) at 3.5 h, with normalization against 16S rRNA. Each experiment was repeated twice with essentially the same results, and a representative blot is shown. Error bars represent standard deviations.

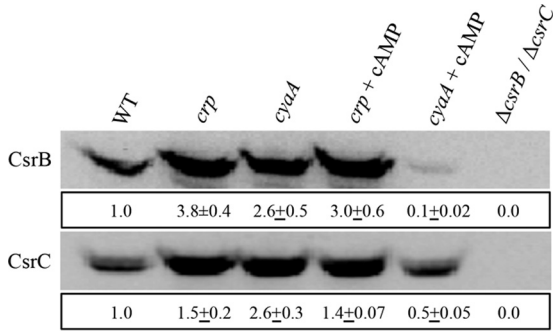

FIG 3 Effect of cAMP (10 mM) addition on CsrB and CsrC levels in LB-MOPS medium. The CsrB or CsrC levels were expressed, after rRNA normalization, with respect to WT (MG1655) after 3 h of growth at 37°C. This experiment was repeated twice with essentially identical results. The means ± ranges are shown for all values. A representative blot is shown.

of carbon. Recall that under these conditions, P-EIIA^{Glc} is unable to bind to CsrD, which decreases the decay rates of CsrB/C (44). Under these conditions, the steady-state levels of CsrB and CsrC in both the *cyaA* and the *crp* mutant were higher than in the isogenic WT strain (Fig. 3). Furthermore, addition of 10 mM cAMP caused a substantial decrease in CsrB/C levels in the *cyaA* mutant but not in a *crp* mutant, confirming that CRP effects on CsrB/C levels require the cAMP-CRP complex.

CRP does not repress CsrB/C expression via effects on CsrA or P-UvrY levels. Normal transcription of both *csrB* and *csrC* depends on P-UvrY, although *csrB* transcription is more highly dependent than that of *csrC* (3, 36, 38). In addition, the RNA helicase DeaD activates UvrY translation, which then activates *csrB*/*C* transcription (62). To test the possibility that CRP functions by altering the level or phosphorylation state of UvrY, we monitored UvrY$_{FLAG}$ protein expressed from the native *uvrY* locus in WT and *crp* mutant strains by Western blotting, as described previously (62). This experiment indicated that the unphosphorylated form of FLAG-tagged UvrY protein was the more abundant form under our experimental conditions (LB-MOPS with 0.2% fructose) (Fig. 4A), as previously observed in LB medium (62). P-UvrY levels were unaltered or slightly lower in the *crp* mutant in the exponential phase and were less than half of the WT levels in the stationary phase of growth. These effects were not consistent with the observed increases in *csrB-lacZ* and *csrC-lacZ* expression (Fig. 1A and C) and in CsrB/CsrC RNA levels (Fig. 2C) seen in the *crp* mutant. Thus, CRP does not negatively regulate CsrB/C levels via effects on UvrY levels or its phosphorylation status. CsrA protein levels were equivalent in the WT and *crp* mutant strains (Fig. 4B),

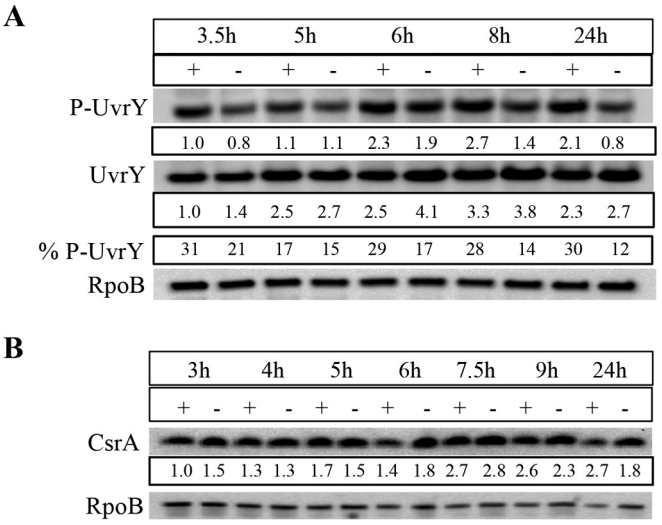

FIG 4 Effect of *crp* mutation on levels of phosphorylated and unphosphorylated UvrY$_{FLAG}$ and CsrA protein. (A) Cultures were grown in LB-MOPS medium with 0.2% fructose and harvested at the indicated time points for preparation of lysates. Proteins (5 μg) were separated by electrophoresis on Phos-Tag gels, transferred to nitrocellulose, and detected with anti-FLAG and anti-RpoB antibodies. % P-UvrY, percentage of P-UvrY with respect to total UvrY protein (P-UvrY plus UvrY after RpoB normalization). (B) Cell lysates were prepared from cultures grown in LB-MOPS medium with 0.2% fructose, and protein (2 μg) was separated on a 12% acrylamide gel, transferred to a PVDF membrane, and detected with anti-CsrA and anti-RpoB antibodies. Proteins from WT (+) and *crp* mutant (−) strains are shown. Each experiment was repeated twice with essentially the same results, and a representative blot is shown.

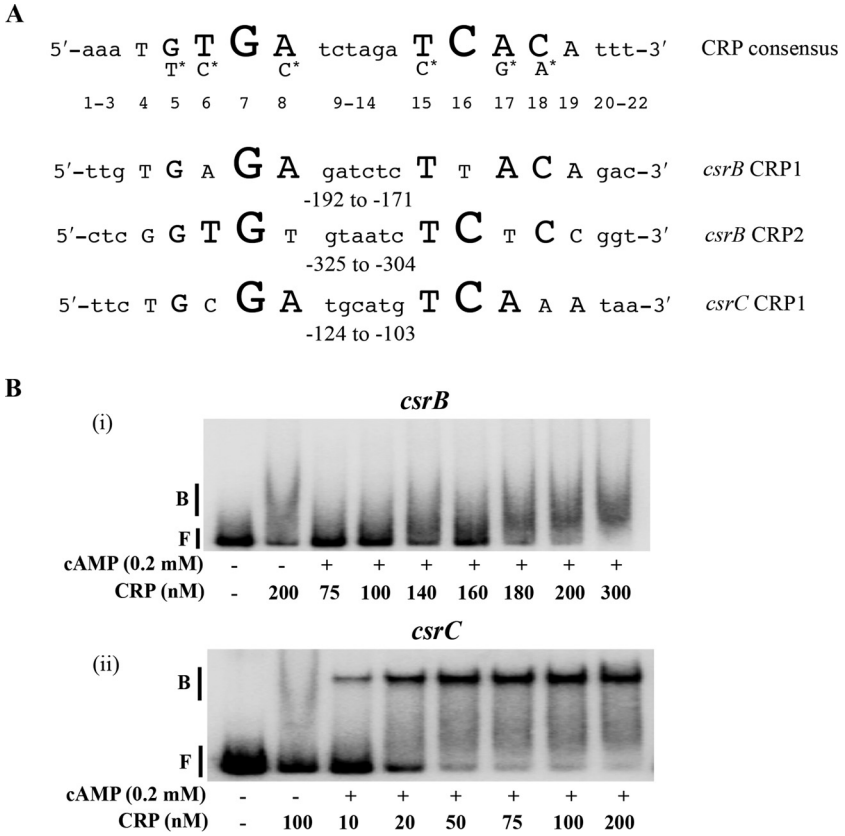

FIG 5 Binding of cAMP-CRP to *csrB* and *csrC* DNA. (A) Consensus sequence for cAMP-CRP binding and predicted binding sites in the upstream flanking regions of *csrB* and *csrC*. Nucleotides in uppercase letters in the *crp* consensus sequence denote the conserved residues, and the size of the nucleotide letters indicates the relative degree of conservation of the nucleotide residue (47). Nucleotides with the asterisk indicate the second most highly conserved residue in comparison to the nucleotide under which they are placed. Numbers indicate the position of each nucleotide relative to the 5′ end of the consensus. Numbers beneath the *csrB* and *csrC* sequences are indicative of location with respect to the transcription initiation site. (B) Electrophoretic gel mobility shift analysis of cAMP-CRP binding to *csrB* and *csrC* DNA. A ^{32}P end-labeled PCR product (0.5 nM) was used in binding reactions performed with or without cAMP (0.2 mM) and CRP, as shown. Positions of free (F) and bound (B) DNA are shown. The apparent K_d for binding of cAMP-CRP to *csrC* DNA was 18 ± 2 nM. Each experiment was conducted twice, and a representative image is shown.

indicating that CRP does not repress CsrB/C through effects on CsrA levels.

cAMP-CRP binds to *csrC* DNA in a region overlapping the P-UvrY binding site. Because P-UvrY and CsrA do not appear to mediate cAMP-CRP effects on *csrB* and *csrC* expression, we hypothesized that cAMP-CRP might directly repress transcription by binding to *csrB* and/or *csrC* DNA. P-UvrY activates transcription of *csrB* and *csrC* by binding to 18-nt inverted repeat (IR) DNA sequences, TGTGAGAGATCTCTTACA and TGTGAGACATTG CCGATA, respectively, centered at nt −183 and −159 from the transcriptional start site (3). CRP binds to a conserved 22-bp DNA sequence (5′-AAATGTGATCTAGATCACATTT-3′) in the regulatory regions of its target genes (57, 58). Possible CRP binding sequences in the upstream regulatory regions of *csrB* and *csrC* were identified using an online tool, Virtual Footprint (www.prodoric.de/vfp). This analysis yielded two potential binding sites for *csrB* (CRP1 and CRP2) and a single site for *csrC* (CRP1) (Fig. 5A). In the case of *csrB*, CRP1 overlaps the P-UvrY binding site, while in the case of *csrC*, CRP1 is immediately downstream of the P-UvrY binding site (Fig. 6) (3).

To determine whether cAMP-CRP binds specifically and with high affinity to the upstream regulatory regions of *csrB* and *csrC*, we first performed electrophoretic gel mobility shift assays (EMSA). Reactions without cAMP were used as a means to address binding specificity. *csrB* DNA showed a shifted complex at a relatively high CRP concentration of ~180 nM (Fig. 5B, panel i). However, the shifted complex was diffuse and there was no difference in the binding of CRP (200 nM) in the presence or absence of cAMP, indicating that binding to CsrB DNA was nonspecific. In contrast, *csrC* DNA formed a distinct shifted complex at a CRP concentration of as low as 10 nM (Fig. 5B, panel ii). Increasing the concentration of CRP resulted in an increasing signal intensity of the shifted complex, with nearly complete binding seen at ~50 nM. In the absence of cAMP, CRP failed to form the distinct complex, confirming that cAMP-CRP bound specifically to *csrC* DNA. The apparent dissociation constant (K_d value) for cAMP-CRP binding to *csrC* DNA was 18 ± 2 nM, similar to that of the lactose and galactose promoters (5 to 10 nM), which are known targets of cAMP-CRP binding (65). EMSA of CRP binding to *csrA*, *uvrY*, and *csrD* DNA in all cases resulted in the formation of diffuse complexes at high CRP concentrations (≥100 nM), similarly to the results seen with *csrB* DNA, indicative of nonspecific binding (data not shown).

To identify the cAMP-CRP and P-UvrY binding site(s) in *csrC*, we performed DNase I footprinting reactions. cAMP-CRP pro-

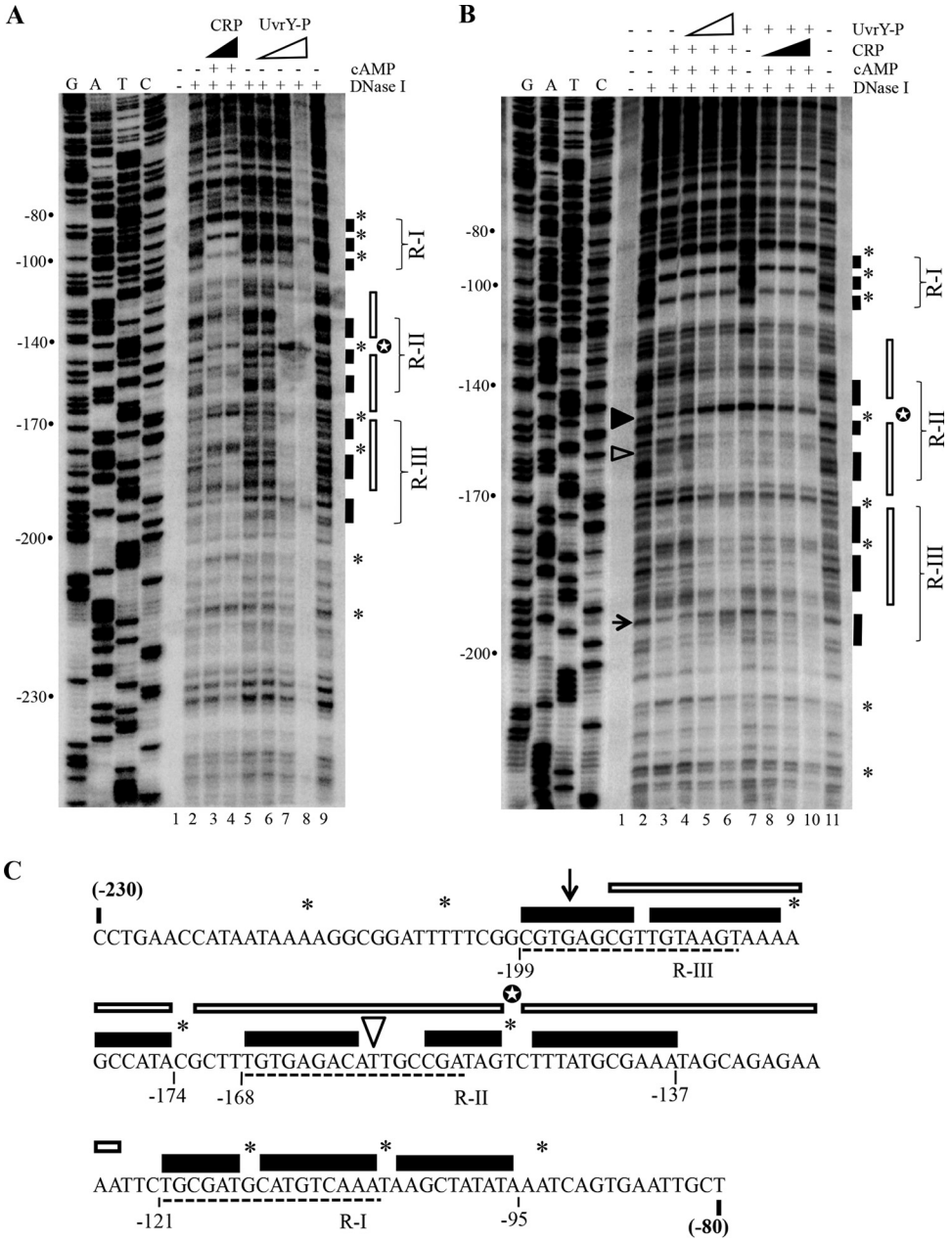

FIG 6 DNase I footprinting of *csrC* DNA in the presence of cAMP-CRP and P-UvrY. (A and B) Lanes G, A, T, and C depict the sequencing ladder. The numbers to the left of the images indicate distance from the transcription start site. Protection by cAMP-CRP and P-UvrY is shown by filled and open bars, respectively. Sites hypersensitive to cleavage in the presence of cAMP-CRP and P-UvrY are indicated by asterisks and a white star, respectively. (A) Footprinting of *csrC* in the presence of CRP or P-UvrY. Reaction mixtures in lanes 3 and 4 contained 100 and 250 nM CRP with 0.2 mM cAMP. Lanes 6, 7, and 8, 250, 500, and 1,000 nM P-UvrY. (B) Footprinting of *csrC* DNA in the presence of cAMP-CRP or P-UvrY or both. Lanes 3 to 6, 100 nM CRP and 0.2 mM cAMP; lanes 4, 5, and 6, 250, 500, and 700 nM P-UvrY; lanes 7 to 10, 500 nM P-UvrY; lanes 8, 9, and 10, 50, 100, and 200 nM CRP with 0.2 mM cAMP. The filled and open arrowheads and the arrow mark the nucleotide residues that were used to assess competition of cAMP-CRP and P-UvrY (the hypersensitive cleavage site caused by P-UvrY binding, a site protected specifically by P-UvrY, and a site protected specifically by cAMP-CRP, respectively). (C) The *csrC* sequence from −230 to −80 with respect to transcription initiation, displaying regions protected by cAMP-CRP and P-UvrY. The regions protected by cAMP-CRP and P-UvrY are indicated by filled and open bars, respectively. Nucleotides marked with an asterisk or a white star represent sites hypersensitive to cleavage in the presence of cAMP-CRP or P-UvrY, respectively. The arrowhead and arrow indicate the single nucleotides used to assess competition. The three regions protected by cAMP-CRP in the DNase I footprinting are indicated by R-I, R-II, and R-III. Sequences underlined with dashed lines are related to the consensus CRP binding sequence (Fig. 5A).

tected three prominent regions (R-I, R-II, and R-III) on *csrC* DNA (Fig. 6A, lanes 3 and 4, and C [marked with filled bars]). R-I included the site predicted by Virtual Footprint (www.prodoric.de/vfp), consisting of the region from nt −95 to −121 relative to the *csrC* transcription start site (Fig. 5A and 6A [lanes 3 and 4] and C). R-I appeared to represent a high-affinity site for binding of cAMP-CRP to *csrC*, since protection occurred at a low concentration of CRP (50 nM) and in the presence of P-UvrY (Fig. 6B, lane

8). cAMP-CRP binding to the two other sites, nt −137 to −168 (R-II) and nt −174 to −199 (R-III), required a higher concentration of CRP (Fig. 6B). Inspection of the nucleotide sequences at R-II and R-III revealed sequences that were related to the conserved nucleotides in the CRP consensus (Fig. 5A and 6C). The binding of cAMP-CRP also led to hypersensitive cleavage at several sites (−93A, −105T, −115G, −149T, −173C, −180A, −205T, and −215A) (Fig. 6, asterisks). DNase I footprinting of *csrC* DNA with P-UvrY showed a protected region from nt −125 to −193 (Fig. 6A, lane 7 [indicated with open bars]), as well as a pronounced hypersensitive cleavage site at −149T. Importantly, the region protected by P-UvrY overlapped the R-II and R-III regions protected by cAMP-CRP.

The results of the DNase I protection studies performed with individual proteins suggested that cAMP-CRP and P-UvrY may compete with each other for binding to *csrC* DNA. To test for binding competition, we first conducted DNase I protection assays in the presence of a constant concentration of cAMP-CRP and increasing concentrations of P-UvrY. In this experiment, the protection pattern of cAMP-CRP at R-II (nt −137 to −168) and R-III (nt −174 to −199) was increasingly replaced by the pattern observed for P-UvrY, including the strong hypersensitive cleavage at −149T (Fig. 6B; compare lanes 3 to 6). In contrast, protection of the R-I site (nt −95 to −121) by CRP was unaffected by the presence of P-UvrY (Fig. 6B, lanes 3 to 6). Alternatively, when increasing amounts of cAMP-CRP were added to reaction mixtures containing a constant amount of P-UvrY, we observed that the lowest concentration of CRP that was tested (50 nM) showed strong protection at the R-I site (nt −95 to −121) (Fig. 6B; compare lanes 7 and 8). Increasing the concentration of CRP (Fig. 6B, lanes 7 to 10) led to the appearance of CRP protection at the R-II site (nt −137 to 168) and the R-III site (nt −174 to −199) and a concomitant decrease in signal intensity of the P-UvrY hypersensitive site at −149T.

We also examined competition at two nucleotide residues (−159T and −196G) which were differentially sensitive to DNase I in the presence of cAMP-CRP versus P-UvrY. Residue −159T was protected by P-UvrY but not by cAMP-CRP. An increase in the concentration of P-UvrY led to increasing protection of this residue (Fig. 6B, lanes 3 to 6), while increasing the concentration of cAMP-CRP resulted in loss of protection at this residue (Fig. 6B, lanes 7 to 10). Similarly, −196G was protected by cAMP-CRP but not by P-UvrY. Increasing the concentration of P-UvrY resulted in decreasing protection of this residue (Fig. 6B, lanes 3 to 6), while increasing the concentration of cAMP-CRP resulted in increasing protection of this residue (Fig. 6B, lanes 7 to 10). These results strengthened the evidence suggesting that cAMP-CRP competes with P-UvrY for binding to *csrC* DNA.

We also conducted DNase I footprinting studies of *csrB* DNA in the presence of P-UvrY and cAMP-CRP (data not shown). As reported previously, P-UvrY protected a region from nt −138 to bp −210 upstream from the *csrB* transcriptional start site (3). cAMP-CRP did not generate a distinct footprint with *csrB* DNA, confirming the findings from EMSA (Fig. 5B) showing that cAMP-CRP does not bind specifically to *csrB* DNA.

cAMP-CRP inhibits *in vitro* expression of *csrC*. Although we were unable to detect expression of *csrB* or *csrC* using *in vitro* transcription reactions with purified components (data not shown), P-UvrY was previously found to directly activate the expression of *csrB-lacZ* and *csrC-lacZ* transcriptional fusions in

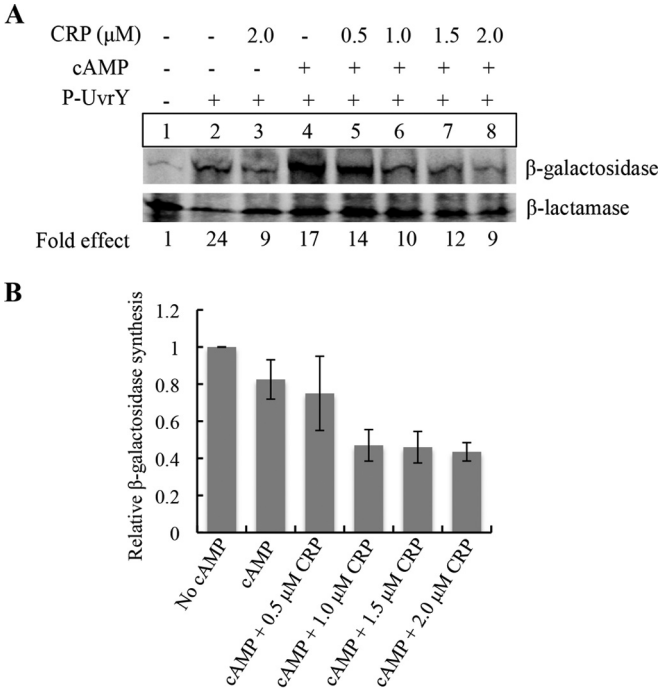

FIG 7 Effect of cAMP-CRP on *in vitro* expression of *csrC-lacZ* in S-30 extracts. (A) An *in vitro* coupled transcription-translation assay was performed using plasmid pLFXcsrC-lacZ (4 μg), P-UvrY (2.3 μM), cAMP (0.2 mM), and CRP as indicated. ^{35}S-methionine-labeled proteins were detected by phosphorimaging, and signal intensity was quantified using Quantity One software. Specific β-galactosidase synthesis values were determined from the β-galactosidase/β-lactamase ratio for each reaction, and fold effects were determined relative to the reaction mixture that lacked CRP, cAMP, and P-UvrY (lane 1). (B) Effect of CRP and cAMP on P-UvrY-dependent *csrC-lacZ* expression. Relative levels of β-galactosidase synthesis were determined by comparing the specific β-galactosidase synthesis values to that of a control reaction (panel A, lane 2). Results depict average values from the results of two independent experiments ± SD.

S-30 transcription-translation assays (36, 38). Thus, we used the latter approach to determine if cAMP-CRP directly represses expression from the *csrC-lacZ* transcriptional fusion in the plasmid pLFXcsrC-lacZ. Addition of phosphorylated UvrY (P-UvrY) alone stimulated β-galactosidase synthesis, as expected (Fig. 7A, lanes 1 and 2). Addition of cAMP alone to the P-UvrY reaction caused a slight (~20%) relative decrease in β-galactosidase synthesis, which was likely due to the presence of endogenous CRP in the S-30 extract (Fig. 7A, lanes 2 and 4, and B). In the presence of cAMP, the addition of increasing CRP concentrations led to decreasing β-galactosidase synthesis relative to the results seen with the β-lactamase gene product (Bla) encoded by pLFXcsrC-lacZ, which served as an internal control (Fig. 7A, lanes 4 to 8). The inhibitory effect began to saturate at a concentration of 1.0 μM CRP, resulting in ~55% inhibition (Fig. 7). This is a minimal estimation of CRP inhibition because it does not include the (~20%) inhibition caused by the endogenous CRP from the S-30 extract (Fig. 7A, lane 2 versus lane 4, and B).

***In vitro* binding of CsrA to *crp* and *cyaA* transcripts.** Transcripts for *crp* and *cyaA* previously copurified with CsrA protein (25). This finding suggested that CsrA might directly regulate *crp* and *cyaA* expression at a posttranscriptional level, resulting in reciprocal interactions among these two global regulatory sys-

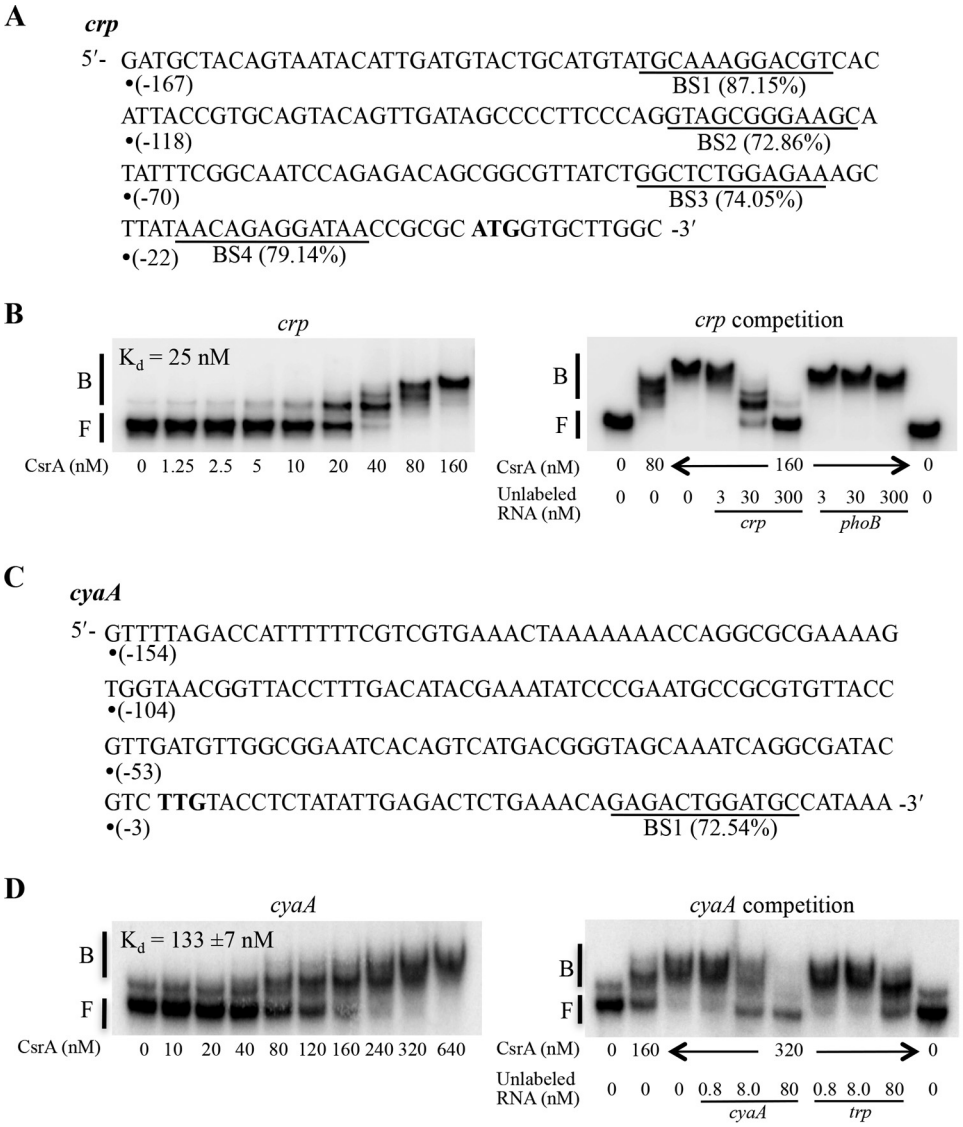

FIG 8 Binding of CsrA to *crp* and *cyaA* transcripts analyzed by EMSA. (A and C) Nucleotide sequences of the untranslated leader and initial coding region of *crp* (A) and *cyaA* (C) RNAs and the predicted sites (underlined) for CsrA binding. The first nucleotide of each sequence (●) is numbered with respect to the translation initiation site. Scores next to each predicted binding site (BS) are based on a position-weight-matrix analysis of CsrA binding sequences (27). The ATG and TTG initiation codons are bolded. (B and D) Binding and competition assays of CsrA with *crp* (B) and *cyaA* (D) transcripts. Positions of free (F) and bound (B) RNA are indicated.

tems. A position-weight matrix (PWM) analysis for potential CsrA binding sequences in the *E. coli* transcriptome (27) suggested that there may be as many as four such sites in the 167-nucleotide untranslated leader of *crp* mRNA (BS1 to BS4) (Fig. 8A). The *cyaA* mRNA leader contains a single potential binding sequence (BS1) in the early coding region (Fig. 8C). Electrophoretic gel mobility shift assays (EMSA) were used to first examine the binding interaction of CsrA with *crp* mRNA. Although major and minor RNA conformers were present in the absence of CsrA, the intensity of a band that ran at a position similar to that of the minor conformer began to increase at ~5 nM CsrA, which is indicative of a CsrA-*crp* RNA complex. This complex became more prominent as the CsrA concentration was increased further (Fig. 8B). A nonlinear least-squares analysis of the data for this binding interaction yielded an apparent dissociation constant (K_d) of 25 nM. At a CsrA concentration of 40 nM, a second shifted complex was observed in addition to the first complex, and little of the RNA remained unbound. At a CsrA concentration of 80 nM, a third shifted complex was observed along with the second complex. A further increase in CsrA concentration to 160 nM led to formation of only the third shifted complex. This series of reactions strongly suggested the binding of multiple CsrA proteins to the *crp* RNA, although this possibility was not further investigated. Unlabeled *crp* RNA was able to compete for the formation of CsrA complexes with the labeled *crp* RNA, while unlabeled *phoB* RNA, which does not bind to CsrA (25), did not compete with *crp* RNA. These findings confirmed that CsrA bound specifically to *crp* RNA (Fig. 8B).

EMSA of *cyaA* RNA showed two RNA species in the absence of CsrA (Fig. 8D), the faster migrating species being the more abundant. CsrA bound similarly to the two species, indicating that they

are two conformers of a single RNA. A shifted complex began to appear at a CsrA concentration of 40 nM and became more prominent as the CsrA concentration was increased further. A nonlinear least-squares analysis of the binding data for this complex yielded an apparent dissociation constant (K_d) of 133 ± 7 nM, indicating that the affinity of CsrA for *cyaA* mRNA was much weaker than for *crp* mRNA. Unlabeled *cyaA* RNA was able to compete for the formation of the CsrA complex with labeled *cyaA* RNA, but unlabeled nonspecific RNA, *Bacillus subtilis trp* mRNA, also competed (Fig. 8D). These results suggested that the binding interaction of CsrA with *cyaA* mRNA might not be specific.

CsrA conditionally affects *crp* and *cyaA* expression at low temperatures. The binding affinity of CsrA for *crp* mRNA (25 nM) was similar to that of several authenticated mRNA targets, e.g., *glgCAP* (39 nM, 4 CsrA binding sites), *pgaABCD* (22 nM, 6 binding sites), *hfq* (38 nM, 1 binding site), *cstA* (40 nM, 4 binding sites), *relA* (17 nM, 6 binding sites), and *csrA* (27 nM, 4 binding sites). Therefore, we decided to examine the effect of CsrA on the *in vivo* expression of a chromosomally integrated *crp′-′lacZ* translational fusion. Although the binding affinity of CsrA to *cyaA* mRNA was weak and presumably nonspecific, we also tested for CsrA effects on a chromosomally integrated *cyaA′-′lacZ* translational fusion. Both fusions were monitored in LB and KB media when cells were grown at 22°C and 37°C. Studies were conducted at 22°C because we found that CsrA activates expression of another *E. coli* gene at 22°C but not at 37°C (L. C. McGibbon, T. Romeo, and P. Babitzke, unpublished results). Growth levels of WT and *csrA* mutant strains in LB and KB media were comparable. At 22°C, expression of the *crp′-′lacZ* fusion in KB medium was lower in the *csrA* mutant at all stages of growth except for early exponential phase, when the level was slightly higher in the *csrA* mutant (Fig. 9A). CsrA had little or no effect on the expression of this fusion in LB medium (Fig. 9B). Expression of the *cyaA′-′lacZ* fusion was moderately lower in the *csrA* mutant in both KB and LB media, but a stronger effect was observed in KB medium at early exponential phase (Fig. 9E and F). The *csrA*::*kan* mutation had negligible effects on the expression of another reporter fusion (*dppA-lacZ*) in KB medium at 22°C (data not shown), suggesting that the observed effects of CsrA on *crp′-′lacZ* and *cyaA′-′lacZ* fusions were specific. No significant effects of CsrA on the expression of either reporter fusion at 37°C in either medium were observed (Fig. 9C, D, G, and H). These findings indicated that CsrA positively affects *crp* and *cyaA* expression in a temperature-dependent fashion.

DISCUSSION

These studies were inspired by observations suggestive of regulatory connections between the catabolite repression and Csr systems. For example, (i) *crp* and *cya* mRNAs copurified with the CsrA protein (25), (ii) potential cAMP-CRP binding sites were identified upstream of the *csrB* gene by bioinformatics analysis (47), and (iii) a number of genes and processes have been reported to be regulated by both CsrA and cAMP-CRP (14, 18, 21, 66) (Fig. 10). In addition, the phosphorylation state of the PTS protein $EIIA^{Glc}$ serves as the key sensory mechanism for cAMP synthesis and catabolite repression control and for the turnover pathway of CsrB/C sRNAs (43, 44, 48). Our present data establish direct and apparently indirect connections between these two important global regulatory systems.

We determined that cAMP-CRP represses the synthesis of *E. coli* CsrB and CsrC sRNAs using a combination of molecular genetics and biochemical evidence. Levels of these sRNAs and *csrB-lacZ* and *csrC-lacZ* expression were elevated in strains unable to produce cAMP-CRP (Fig. 1 to 3). While both CsrB and CsrC responded positively to cAMP-CRP *in vivo*, only *csrC* DNA was a target of specific, high-affinity *in vitro* binding by cAMP-CRP (Fig. 5 to 8). Thus, cAMP-CRP uses distinct mechanisms for regulating *csrB* versus *csrC* expression. Consistent with this finding, cAMP-CRP had little or no effect on the cellular levels of P-UvrY and CsrA, which are known to activate both *csrB* and *csrC* expression (Fig. 4). Integration host factor IHF is the only factor known to differentially activate *csrB* transcription without affecting *csrC* (3, 41). However, the *ihfA* and *ihfB* genes, which encode the IHF subunits, were not among the *E. coli* genes found to contain cAMP-CRP binding sites by genomic SELEX analyses (47). Thus, IHF seems unlikely to mediate the effects of cAMP-CRP on *csrB*.

The Csr regulon is broad in scope and includes many genes involved in carbon and energy metabolism. Not surprisingly, the carbon nutritional status influences the workings of the Csr system. The BarA-UvrY (-SirA) TCS of *E. coli* and *Salmonella* activates *csrB* expression in response to end products of bacterial carbon metabolism that accumulate in the mammalian large intestine, such as formate, acetate, and propionate (39, 67). Furthermore, chromatin immunoprecipitation-exo (ChIP-exo) studies have shown that P-UvrY (P-SirA) binds primarily to *csrB* and *csrC* DNA *in vivo* in these bacteria, indicating that activation of *csrB* and *csrC* transcription is the main function of BarA-UvrY (3). In contrast, citrate accumulation in *Vibrio fischeri* (68) and other tricarboxylic acid cycle intermediates in *Pseudomonas fluorescens* (69) are correlated with the function of this TCS, also referred to as GacS-GacA. The biochemical mechanisms involved in these sensory processes remain to be determined. In *E. coli*, CsrA positively regulates several enzymes of glycolysis, in particular, the enzyme phosphofructokinase A, which drives metabolic flux beyond the upper trunk of the glycolysis pathway (7, 13). By inference, products of carbon metabolism downregulate CsrA activity and glycolytic flux through the Embeden-Meyerhof-Parnas pathway, while they activate gluconeogenesis, glycogen synthesis, synthesis of the biofilm exopolysaccharide dPNAG, and pathways and processes favoring stress resistance and survival, which are repressed by CsrA (Fig. 10) (7, 17, 18, 22, 24, 33).

The Csr system is also regulated in complex ways by the availability of preferred carbon substrate for growth (Fig. 10). Transport of glucose by the PTS pathway leads to dephosphorylation of $EIIA^{Glc}$, which binds to CsrD and activates the decay pathway for CsrB/C in *E. coli* (43, 44). This kind of regulatory pathway may function in most *Enterobacteriaceae*, *Vibrionaceae*, and *Shewanellaceae* species and yet is absent in the majority of gammaproteobacterial families, the members of which lack a *csrD* homolog (42, 43). Furthermore, cAMP-CRP modestly inhibits CsrB/C decay (Fig. 2). Therefore, $EIIA^{Glc}$ and P-$EIIA^{Glc}$ relay complementary information to CsrD and adenylate cyclase, respectively, favoring CsrB/C decay when glucose is present. Together, *csrB/C* transcription, which is stimulated by end products of carbon metabolism, and CsrB/C decay, which is activated by glucose, have the potential to reinforce each other's effects on CsrB/C. Both pathways should drive CsrB/C accumulation when preferred carbon resources have been expended and end products have accumulated, promoting the physiological switch from glycolytic growth to stationary-phase metabolism (9, 44).

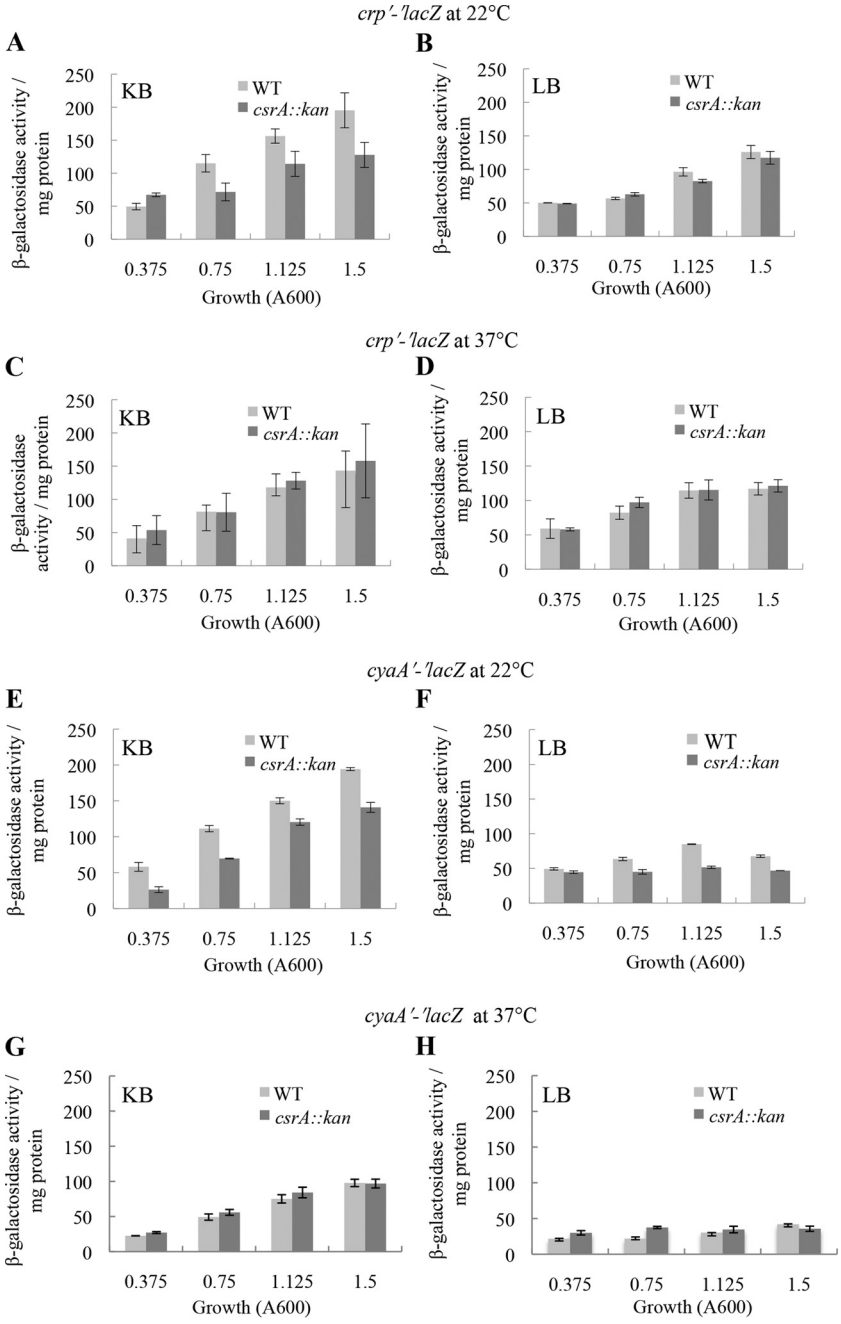

FIG 9 Effect of *csrA*::*kan* disruption on *in vivo* expression of *crp'-'lacZ* and *cyaA'-'lacZ* translational fusions in KB (A, C, E, and G) and LB medium (B, D, F, and H) at 22°C or 37°C, as shown. The results represent the averages of the results of two independent experiments, and error bars depict standard deviations. Growth levels of CF7789 (WT) and its isogenic *csrA*::*kan* strain were similar in KB medium and LB medium under the growth conditions employed for the assay.

Our new observations present a twist on the role of carbon substrate in the Csr system. cAMP-CRP formation, which is inhibited by the effect of glucose on $EIIA^{Glc}$ phosphorylation, leads to repression of *csrB/C* transcription (Fig. 1). Thus, the presence of glucose has the potential to activate both the synthesis and turnover of CsrB/C, through its effects on the phosphorylation state of $EIIA^{Glc}$ (Fig. 10). How might these conflicting effects of glucose be of benefit to *E. coli*? When a preferred carbon source is present and metabolic end products such as formate or acetate are accumulating, both the synthesis and turnover of CsrB/C should occur. We propose that this may lead to accelerated responses to cues or stimuli affecting the Csr system, as described in general for the behavior of incoherent feedback loops (53, 70). In support of this hypothesis, results of modeling studies with genes of the Csr system suggest that the CsrD-dependent decay pathway for CsrB/C sRNAs enhances rates of Csr response to signals, although the involvement of glucose or carbon metabolites in this process has not been demonstrated (71). In view of the hundreds of genes and numerous pathways and processes that are controlled by CsrA (13, 25, 33), the proposed operation of a futile cycle of CsrB/C

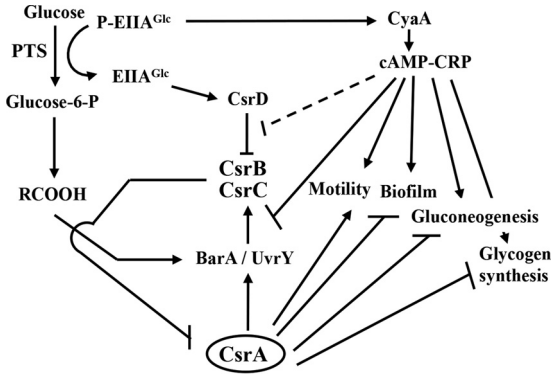

FIG 10 A model for the impact of carbon nutrition on Csr circuitry. Availability of carbon nutrition and end product accumulation impact the workings of the Csr system. During glucose transport, EIIA^{Glc} of the PTS becomes relatively dephosphorylated and is able to bind to CsrD only in this form, activating CsrB/C decay (42–44). End products of metabolism (RCOOH) such as formate and acetate (RCOOH) activate *csrB/C* transcription via the BarA-UvrY TCS (39). Thus, the depletion of carbon substrate and accumulation of end products cause CsrB/C accumulation and subsequent inhibition of CsrA activity. In turn, CsrA indirectly activates *csrB/C* transcription, creating a negative-feedback loop that supports rapid response dynamics of the system (3, 36–39, 71). Inhibition of CsrA decreases expression of glycolytic genes and increases expression of genes for gluconeogenesis, glycogen biosynthesis, biofilm formation, and adaptation to stationary-phase and stress conditions (7, 14, 18, 21, 63). In the absence of a preferred carbon source, P-EIIA^{Glc} binds to adenylate cyclase (CyaA), activating cAMP synthesis and cAMP-CRP formation (48), which represses transcription of *csrC* directly (Fig. 1 to 3 and 5 to 7) and of *csrB* indirectly (Fig. 1 to 3 and 5). The latter distinct effects of CsrA on *csrB* and *csrC* are shown as a combined inhibitory interaction. The results of our present studies imply that a futile cycle of CsrB/C synthesis and turnover may occur when glucose is abundant and end products begin to accumulate, with the potential to poise the Csr system for rapid response to shifting regulatory cues. A broken line indicates that cAMP-CRP has weak (2-fold) effects on CsrB/C decay. Additional details of this circuitry are discussed in the text.

synthesis and turnover when a preferred carbon source is available may be a small price to pay to poise the Csr system for rapid response.

We demonstrated that cAMP-CRP directly represses *csrC* expression by binding to *csrC* DNA (Fig. 5, 6, and 8), while *csrB* appears to be repressed indirectly (Fig. 5 and 7). Repression by cAMP-CRP can be accomplished in a number of ways. For example, CRP can bind at a location close to the promoter and directly interfere with transcription initiation or elongation (57, 72). Alternatively, CRP can prevent binding of an activator (52) or can activate transcription from a promoter and indirectly lead to repression of transcription from an overlapping divergent promoter (73, 74). Our results suggest that repression of *csrC* expression by cAMP-CRP acts in conjunction with P-UvrY-dependent activation. DNase I footprinting experiments show that cAMP-CRP and P-UvrY compete for binding in a region far upstream of the *csrC* promoter (Fig. 6). We should emphasize that cAMP-CRP binds even more tightly at a location immediately downstream of the P-UvrY binding site (Fig. 6). Whether repression is mediated by direct competition of cAMP-CRP with P-UvrY for binding to *csrC* DNA or is a consequence of cAMP-CRP binding to the downstream site and inhibiting the productive interaction of bound P-UvrY with RNA polymerase or other regulatory elements for *csrC* transcription remains to be seen.

The Csr system appears to be conserved in all *Gammaproteobacteria* species, but details such as the number of CsrA paralogs and Csr sRNAs produced by a given species can differ (6, 44, 75, 76). Not surprisingly, even among closely related *Enterobacteriaceae* species, the links between Csr and catabolite repression circuitry differ. In *Yersinia pseudotuberculosis*, cAMP-CRP exerts indirect and opposite regulatory effects on *csrB* and *csrC* (77). Furthermore, while *csrB* expression in *Y. pseudotuberculosis* depends on BarA-UvrY, *csrC* expression is directly activated by the PhoP-PhoQ TCS (78). *Salmonella enterica* was reported to somehow activate expression of the *uvrY* ortholog, *sirA*, via cAMP-CRP, with positive downstream effects on *csrB-lacZ* and *csrC-lacZ* gene fusions (79). In addition, CLIP-seq studies in *Salmonella* revealed binding of CsrA to *crp* (*cap*) leader mRNA at two locations (80), one of which is related in sequence to *E. coli* BS2 (Fig. 8A). Additional studies will be required to unravel the biological significance of such variations in the Csr and catabolite repression networks.

ACKNOWLEDGMENTS

This study was supported by grants to T.R. and P.B. (NIH GM059969) and D.G. (CONACyT 178033).

FUNDING INFORMATION

This work, including the efforts of Paul Babitzke and Tony Romeo, was funded by HHS | NIH | NIH Office of the Director (OD) (GM059969). This work, including the efforts of Dimitris Georgellis, was funded by Consejo Nacional de Ciencia y Tecnología (CONACYT) (178033).

REFERENCES

1. **White D, Hart ME, Romeo T.** 1996. Phylogenetic distribution of the global regulatory gene *csrA* among eubacteria. Gene **182:**221–223. http://dx.doi.org/10.1016/S0378-1119(96)00547-1.
2. **Mercante J, Suzuki K, Cheng X, Babitzke P, Romeo T.** 2006. Comprehensive alanine-scanning mutagenesis of *Escherichia coli* CsrA defines two subdomains of critical functional importance. J Biol Chem **281:**31832–31842. http://dx.doi.org/10.1074/jbc.M606057200.
3. **Zere TR, Vakulskas CA, Leng Y, Pannuri A, Potts AH, Dias R, Tang D, Kolaczkowski B, Georgellis D, Ahmer BM, Romeo T.** 2015. Genomic targets and features of BarA-UvrY (-SirA) signal transduction systems. PLoS One **10:**e0145035. http://dx.doi.org/10.1371/journal.pone.0145035.
4. **Romeo T, Vakulskas CA, Babitzke P.** 2013. Post-transcriptional regulation on a global scale: form and function of Csr/Rsm systems. Environ Microbiol **15:**313–324. http://dx.doi.org/10.1111/j.1462-2920.2012.02794.x.
5. **Babitzke P, Baker CS, Romeo T.** 2009. Regulation of translation initiation by RNA binding proteins. Annu Rev Microbiol **63:**27–44. http://dx.doi.org/10.1146/annurev.micro.091208.073514.
6. **Vakulskas CA, Potts AH, Babitzke P, Ahmer BM, Romeo T.** 2015. Regulation of bacterial virulence by Csr (Rsm) systems. Microbiol Mol Biol Rev **79:**193–224. http://dx.doi.org/10.1128/MMBR.00052-14.
7. **Sabnis NA, Yang H, Romeo T.** 1995. Pleiotropic regulation of central carbohydrate metabolism in *Escherichia coli* via the gene *csrA*. J Biol Chem **270:**29096–29104. http://dx.doi.org/10.1074/jbc.270.49.29096.
8. **Revelles O, Millard P, Nougayrede JP, Dobrindt U, Oswald E, Letisse F, Portais JC.** 2013. The carbon storage regulator (Csr) system exerts a nutrient-specific control over central metabolism in *Escherichia coli* strain Nissle 1917. PLoS One **8:**e66386. http://dx.doi.org/10.1371/journal.pone.0066386.
9. **Pernestig AK, Georgellis D, Romeo T, Suzuki K, Tomenius H, Normark S, Melefors O.** 2003. The *Escherichia coli* BarA-UvrY two-component system is needed for efficient switching between glycolytic and gluconeogenic carbon sources. J Bacteriol **185:**843–853. http://dx.doi.org/10.1128/JB.185.3.843-853.2003.
10. **Murray EL, Conway T.** 2005. Multiple regulators control expression of the Entner-Doudoroff aldolase (Eda) of *Escherichia coli*. J Bacteriol **187:**991–1000. http://dx.doi.org/10.1128/JB.187.3.991-1000.2005.
11. **Wei B, Shin S, LaPorte D, Wolfe AJ, Romeo T.** 2000. Global regulatory mutations in *csrA* and *rpoS* cause severe central carbon stress in *Escherichia coli* in the presence of acetate. J Bacteriol **182:**1632–1640. http://dx.doi.org/10.1128/JB.182.6.1632-1640.2000.

12. **Patterson-Fortin LM, Vakulskas CA, Yakhnin H, Babitzke P, Romeo T.** 2013. Dual posttranscriptional regulation via a cofactor-responsive mRNA leader. J Mol Biol **425:**3662–3677. http://dx.doi.org/10.1016/j.jmb.2012.12.010.
13. **Morin M, Ropers D, Letisse F, Laguerre S, Portais JC, Cocaign-Bousquet M, Enjalbert B.** 2016. The post-transcriptional regulatory system CSR controls the balance of metabolic pools in upper glycolysis of *Escherichia coli*. Mol Microbiol **100:**686–700. http://dx.doi.org/10.1111/mmi.13343.
14. **Wei BL, Brun-Zinkernagel AM, Simecka JW, Pruss BM, Babitzke P, Romeo T.** 2001. Positive regulation of motility and *flhDC* expression by the RNA-binding protein CsrA of *Escherichia coli*. Mol Microbiol **40:**245–256. http://dx.doi.org/10.1046/j.1365-2958.2001.02380.x.
15. **Yakhnin AV, Baker CS, Vakulskas CA, Yakhnin H, Berezin I, Romeo T, Babitzke P.** 2013. CsrA activates *flhDC* expression by protecting *flhDC* mRNA from RNase E-mediated cleavage. Mol Microbiol **87:**851–866. http://dx.doi.org/10.1111/mmi.12136.
16. **Liu MY, Yang H, Romeo T.** 1995. The product of the pleiotropic *Escherichia coli* gene *csrA* modulates glycogen biosynthesis via effects on mRNA stability. J Bacteriol **177:**2663–2672.
17. **Yang H, Liu MY, Romeo T.** 1996. Coordinate genetic regulation of glycogen catabolism and biosynthesis in *Escherichia coli* via the CsrA gene product. J Bacteriol **178:**1012–1017.
18. **Romeo T, Gong M, Liu MY, Brun-Zinkernagel AM.** 1993. Identification and molecular characterization of *csrA*, a pleiotropic gene from *Escherichia coli* that affects glycogen biosynthesis, gluconeogenesis, cell size, and surface properties. J Bacteriol **175:**4744–4755.
19. **Baker CS, Morozov I, Suzuki K, Romeo T, Babitzke P.** 2002. CsrA regulates glycogen biosynthesis by preventing translation of *glgC* in *Escherichia coli*. Mol Microbiol **44:**1599–1610. http://dx.doi.org/10.1046/j.1365-2958.2002.02982.x.
20. **Mercante J, Edwards AN, Dubey AK, Babitzke P, Romeo T.** 2009. Molecular geometry of CsrA (RsmA) binding to RNA and its implications for regulated expression. J Mol Biol **392:**511–528. http://dx.doi.org/10.1016/j.jmb.2009.07.034.
21. **Jackson DW, Suzuki K, Oakford L, Simecka JW, Hart ME, Romeo T.** 2002. Biofilm formation and dispersal under the influence of the global regulator CsrA of *Escherichia coli*. J Bacteriol **184:**290–301. http://dx.doi.org/10.1128/JB.184.1.290-301.2002.
22. **Wang X, Dubey AK, Suzuki K, Baker CS, Babitzke P, Romeo T.** 2005. CsrA post-transcriptionally represses *pgaABCD*, responsible for synthesis of a biofilm polysaccharide adhesin of *Escherichia coli*. Mol Microbiol **56:**1648–1663. http://dx.doi.org/10.1111/j.1365-2958.2005.04648.x.
23. **Jonas K, Edwards AN, Simm R, Romeo T, Romling U, Melefors O.** 2008. The RNA binding protein CsrA controls cyclic di-GMP metabolism by directly regulating the expression of GGDEF proteins. Mol Microbiol **70:**236–257. http://dx.doi.org/10.1111/j.1365-2958.2008.06411.x.
24. **Pannuri A, Yakhnin H, Vakulskas CA, Edwards AN, Babitzke P, Romeo T.** 2012. Translational repression of NhaR, a novel pathway for multi-tier regulation of biofilm circuitry by CsrA. J Bacteriol **194:**79–89. http://dx.doi.org/10.1128/JB.06209-11.
25. **Edwards AN, Patterson-Fortin LM, Vakulskas CA, Mercante JW, Potrykus K, Vinella D, Camacho MI, Fields JA, Thompson SA, Georgellis D, Cashel M, Babitzke P, Romeo T.** 2011. Circuitry linking the Csr and stringent response global regulatory systems. Mol Microbiol **80:**1561–1580. http://dx.doi.org/10.1111/j.1365-2958.2011.07663.x.
26. **Dubey AK, Baker CS, Suzuki K, Jones AD, Pandit P, Romeo T, Babitzke P.** 2003. CsrA regulates translation of the *Escherichia coli* carbon starvation gene, *cstA*, by blocking ribosome access to the *cstA* transcript. J Bacteriol **185:**4450–4460. http://dx.doi.org/10.1128/JB.185.15.4450-4460.2003.
27. **Baker CS, Eory LA, Yakhnin H, Mercante J, Romeo T, Babitzke P.** 2007. CsrA inhibits translation initiation of *Escherichia coli hfq* by binding to a single site overlapping the Shine-Dalgarno sequence. J Bacteriol **189:**5472–5481. http://dx.doi.org/10.1128/JB.00529-07.
28. **Yang TY, Sung YM, Lei GS, Romeo T, Chak KF.** 2010. Posttranscriptional repression of the *cel* gene of the ColE7 operon by the RNA-binding protein CsrA of *Escherichia coli*. Nucleic Acids Res **38:**3936–3951. http://dx.doi.org/10.1093/nar/gkq177.
29. **Yakhnin H, Baker CS, Berezin I, Evangelista MA, Rassin A, Romeo T, Babitzke P.** 2011. CsrA represses translation of *sdiA*, which encodes the N-acylhomoserine-L-lactone receptor of *Escherichia coli*, by binding exclusively within the coding region of *sdiA* mRNA. J Bacteriol **193:**6162–6170. http://dx.doi.org/10.1128/JB.05975-11.
30. **Figueroa-Bossi N, Schwartz A, Guillemardet B, D'Heygere F, Bossi L, Boudvillain M.** 2014. RNA remodeling by bacterial global regulator CsrA promotes Rho-dependent transcription termination. Genes Dev **28:**1239–1251. http://dx.doi.org/10.1101/gad.240192.114.
31. **Bhatt S, Edwards AN, Nguyen HT, Merlin D, Romeo T, Kalman D.** 2009. The RNA binding protein CsrA is a pleiotropic regulator of the locus of enterocyte effacement pathogenicity island of enteropathogenic *Escherichia coli*. Infect Immun **77:**3552–3568. http://dx.doi.org/10.1128/IAI.00418-09.
32. **Bhatt S, Romeo T, Kalman D.** 2011. Honing the message: post-transcriptional and post-translational control in attaching and effacing pathogens. Trends Microbiol **19:**217–224. http://dx.doi.org/10.1016/j.tim.2011.01.004.
33. **Esquerré T, Bouvier M, Turlan C, Carpousis AJ, Girbal L, Cocaign-Bousquet M.** 2016. The Csr system regulates genome-wide mRNA stability and transcription and thus gene expression in *Escherichia coli*. Sci Rep **6:**25057. http://dx.doi.org/10.1038/srep25057.
34. **Yakhnin H, Yakhnin AV, Baker CS, Sineva E, Berezin I, Romeo T, Babitzke P.** 2011. Complex regulation of the global regulatory gene *csrA*: CsrA-mediated translational repression, transcription from five promoters by $E\sigma^{70}$ and $E\sigma(S)$, and indirect transcriptional activation by CsrA. Mol Microbiol **81:**689–704. http://dx.doi.org/10.1111/j.1365-2958.2011.07723.x.
35. **Liu MY, Romeo T.** 1997. The global regulator CsrA of *Escherichia coli* is a specific mRNA-binding protein. J Bacteriol **179:**4639–4642.
36. **Weilbacher T, Suzuki K, Dubey AK, Wang X, Gudapaty S, Morozov I, Baker CS, Georgellis D, Babitzke P, Romeo T.** 2003. A novel sRNA component of the carbon storage regulatory system of *Escherichia coli*. Mol Microbiol **48:**657–670. http://dx.doi.org/10.1046/j.1365-2958.2003.03459.x.
37. **Camacho MI, Alvarez AF, Chavez RG, Romeo T, Merino E, Georgellis D.** 2015. Effects of the global regulator CsrA on the BarA/UvrY two-component signaling system. J Bacteriol **197:**983–991. http://dx.doi.org/10.1128/JB.02325-14.
38. **Suzuki K, Wang X, Weilbacher T, Pernestig AK, Melefors O, Georgellis D, Babitzke P, Romeo T.** 2002. Regulatory circuitry of the CsrA/CsrB and BarA/UvrY systems of *Escherichia coli*. J Bacteriol **184:**5130–5140. http://dx.doi.org/10.1128/JB.184.18.5130-5140.2002.
39. **Chavez RG, Alvarez AF, Romeo T, Georgellis D.** 2010. The physiological stimulus for the BarA sensor kinase. J Bacteriol **192:**2009–2012. http://dx.doi.org/10.1128/JB.01685-09.
40. **Martínez LC, Yakhnin H, Camacho MI, Georgellis D, Babitzke P, Puente JL, Bustamante VH.** 2011. Integration of a complex regulatory cascade involving the SirA/BarA and Csr global regulatory systems that controls expression of the *Salmonella* SPI-1 and SPI-2 virulence regulons through HilD. Mol Microbiol **80:**1637–1656. http://dx.doi.org/10.1111/j.1365-2958.2011.07674.x.
41. **Martínez LC, Martínez-Flores I, Salgado H, Fernández-Mora M, Medina-Rivera A, Puente JL, Collado-Vides J, Bustamante VH.** 2014. In silico identification and experimental characterization of regulatory elements controlling the expression of the *Salmonella csrB* and *csrC* genes. J Bacteriol **196:**325–336. http://dx.doi.org/10.1128/JB.00806-13.
42. **Suzuki K, Babitzke P, Kushner SR, Romeo T.** 2006. Identification of a novel regulatory protein (CsrD) that targets the global regulatory RNAs CsrB and CsrC for degradation by RNase E. Genes Dev **20:**2605–2617. http://dx.doi.org/10.1101/gad.1461606.
43. **Vakulskas CA, Leng Y, Abe H, Amaki T, Okayama A, Babitzke P, Suzuki K, Romeo T.** 2016. Antagonistic control of the turnover pathway for the global regulatory sRNA CsrB by the CsrA and CsrD proteins. Nucleic Acids Res http://dx.doi.org/10.1093/nar/gkw484.
44. **Leng Y, Vakulskas CA, Zere TR, Pickering BS, Watnick PI, Babitzke P, Romeo T.** 2016. Regulation of CsrB/C sRNA decay by $EIIA^{Glc}$ of the phosphoenolpyruvate:carbohydrate phosphotransferase system. Mol Microbiol **99:**627–639. http://dx.doi.org/10.1111/mmi.13259.
45. **Gosset G, Zhang Z, Nayyar S, Cuevas WA, Saier MH, Jr.** 2004. Transcriptome analysis of CRP-dependent catabolite control of gene expression in *Escherichia coli*. J Bacteriol **186:**3516–3524. http://dx.doi.org/10.1128/JB.186.11.3516-3524.2004.
46. **Gutierrez-Ríos RM, Freyre-Gonzalez JA, Resendis O, Collado-Vides J, Saier M, Gosset G.** 2007. Identification of regulatory network topological units coordinating the genome-wide transcriptional response to glucose in *Escherichia coli*. BMC Microbiol **7:**53. http://dx.doi.org/10.1186/1471-2180-7-53.

47. **Shimada T, Fujita N, Yamamoto K, Ishihama A.** 2011. Novel roles of cAMP receptor protein (CRP) in regulation of transport and metabolism of carbon sources. PLoS One **6:**e20081. http://dx.doi.org/10.1371/journal.pone.0020081.
48. **Deutscher J, Ake FM, Derkaoui M, Zebre AC, Cao TN, Bouraoui H, Kentache T, Mokhtari A, Milohanic E, Joyet P.** 2014. The bacterial phosphoenolpyruvate:carbohydrate phosphotransferase system: regulation by protein phosphorylation and phosphorylation-dependent protein-protein interactions. Microbiol Mol Biol Rev **78:**231–256. http://dx.doi.org/10.1128/MMBR.00001-14.
49. **Görke B, Stülke J.** 2008. Carbon catabolite repression in bacteria: many ways to make the most out of nutrients. Nat Rev Microbiol **6:**613–624. http://dx.doi.org/10.1038/nrmicro1932.
50. **De Lay N, Gottesman S.** 2009. The CRP-activated small noncoding regulatory RNA CyaR (RyeE) links nutritional status to group behavior. J Bacteriol **191:**461–476. http://dx.doi.org/10.1128/JB.01157-08.
51. **Papenfort K, Pfeiffer V, Lucchini S, Sonawane A, Hinton JC, Vogel J.** 2008. Systematic deletion of Salmonella small RNA genes identifies CyaR, a conserved CRP-dependent riboregulator of OmpX synthesis. Mol Microbiol **68:**890–906. http://dx.doi.org/10.1111/j.1365-2958.2008.06189.x.
52. **Polayes DA, Rice PW, Garner MM, Dahlberg JE.** 1988. Cyclic AMP-cyclic AMP receptor protein as a repressor of transcription of the *spf* gene of *Escherichia coli*. J Bacteriol **170:**3110–3114.
53. **Beisel CL, Storz G.** 2011. The base-pairing RNA spot 42 participates in a multioutput feedforward loop to help enact catabolite repression in *Escherichia coli*. Mol Cell **41:**286–297. http://dx.doi.org/10.1016/j.molcel.2010.12.027.
54. **Thomason MK, Fontaine F, De Lay N, Storz G.** 2012. A small RNA that regulates motility and biofilm formation in response to changes in nutrient availability in *Escherichia coli*. Mol Microbiol **84:**17–35. http://dx.doi.org/10.1111/j.1365-2958.2012.07965.x.
55. **Grainger DC, Hurd D, Harrison M, Holdstock J, Busby SJ.** 2005. Studies of the distribution of *Escherichia coli* cAMP-receptor protein and RNA polymerase along the *E. coli* chromosome. Proc Natl Acad Sci U S A **102:**17693–17698. http://dx.doi.org/10.1073/pnas.0506687102.
56. **You C, Okano H, Hui S, Zhang Z, Kim M, Gunderson CW, Wang YP, Lenz P, Yan D, Hwa T.** 2013. Coordination of bacterial proteome with metabolism by cyclic AMP signalling. Nature **500:**301–306. http://dx.doi.org/10.1038/nature12446.
57. **Kolb A, Busby S, Buc H, Garges S, Adhya S.** 1993. Transcriptional regulation by cAMP and its receptor protein. Annu Rev Biochem **62:**749–795. http://dx.doi.org/10.1146/annurev.bi.62.070193.003533.
58. **Busby S, Ebright RH.** 1999. Transcription activation by catabolic activator protein (CAP). J Mol Biol **293:**199–213. http://dx.doi.org/10.1006/jmbi.1999.3161.
59. **Miller J.** 1972. Experiments in molecular genetics. Cold Spring Harbor Laboratory, Cold Spring Harbor, NY.
60. **Haldimann A, Wanner BL.** 2001. Conditional-replication, excision and retrieval plasmid-host systems for gene structure-function studies of bacteria. J Bacteriol **183:**6384–6393. http://dx.doi.org/10.1128/JB.183.21.6384-6393.2001.
61. **Romeo T, Black J, Preiss J.** 1990. Genetic regulation of glycogen synthesis in *Escherichia coli*: *in vivo* effects of the catabolic repression and stringent response systems in *glg* gene expression. Curr Microbiol **21:**131–137. http://dx.doi.org/10.1007/BF02091831.
62. **Vakulskas CA, Pannuri A, Cortes-Selva D, Zere TR, Ahmer BM, Babitzke P, Romeo T.** 2014. Global effects of the DEAD-box RNA helicase DeaD (CsdA) on gene expression over a broad range of temperatures. Mol Microbiol **92:**945–958. http://dx.doi.org/10.1111/mmi.12606.
63. **Wickstrum JR, Egan SM.** 2002. Ni^{+}-affinity purification of untagged cAMP receptor protein. Biotechniques **33:**728–730.
64. **Hogema BM, Arents JC, Bader R, Eijkemans K, Yoshida H, Takahashi H, Aiba H, Postma PW.** 1998. Inducer exclusion in *Escherichia coli* by non-PTS substrates: the role of the PEP to pyruvate ratio in determining the phosphorylation state of enzyme IIA^{Glc}. Mol Microbiol **30:**487–498. http://dx.doi.org/10.1046/j.1365-2958.1998.01053.x.
65. **Kolb A, Busby S, Herbert M, Kotlarz D, Buc H.** 1983. Comparison of the binding sites for the *Escherichia coli* cAMP receptor protein at the lactose and galactose promoters. EMBO J **2:**217–222.
66. **Jackson DW, Simecka JW, Romeo T.** 2002. Catabolite repression of *Escherichia coli* biofilm formation. J Bacteriol **184:**3406–3410. http://dx.doi.org/10.1128/JB.184.12.3406-3410.2002.
67. **Lawhon SD, Maurer R, Suyemoto M, Altier C.** 2002. Intestinal short-chain fatty acids alter *Salmonella typhimurium* invasion gene expression and virulence through BarA/SirA. Mol Microbiol **46:**1451–1464. http://dx.doi.org/10.1046/j.1365-2958.2002.03268.x.
68. **Septer AN, Bose JL, Lipzen A, Martin J, Whistler C, Stabb EV.** 2015. Bright luminescence of *Vibrio fischeri* aconitase mutants reveals a connection between citrate and the Gac/Csr regulatory system. Mol Microbiol **95:**283–296. http://dx.doi.org/10.1111/mmi.12864.
69. **Takeuchi K, Kiefer P, Reimmann C, Keel C, Dubuis C, Rotli J, Vorholt JA, Haas D.** 2009. Small RNA dependent expression of secondary metabolism is controlled by Krebs cycle function in *Pseudomonas fluorescens*. J Biol Chem **284:**34976–34985. http://dx.doi.org/10.1074/jbc.M109.052571.
70. **Mangan S, Alon U.** 2003. Structure and function of the feed-forward loop network motif. Proc Natl Acad Sci U S A **100:**11980–11985. http://dx.doi.org/10.1073/pnas.2133841100.
71. **Adamson DN, Lim HN.** 2013. Rapid and robust signaling in the CsrA cascade via RNA-protein interactions and feedback regulation. Proc Natl Acad Sci U S A **110:**13120–13125. http://dx.doi.org/10.1073/pnas.1308476110.
72. **Nakano M, Ogasawara H, Shimada T, Yamamoto K, Ishihama A.** 2014. Involvement of cAMP-CRP in transcription activation and repression of the *pck* gene encoding PEP carboxykinase, the key enzyme of gluconeogenesis. FEMS Microbiol Lett **355:**93–99. http://dx.doi.org/10.1111/1574-6968.12466.
73. **Hanamura A, Aiba H.** 1991. Molecular mechanism of negative autoregulation of *Escherichia coli crp* gene. Nucleic Acids Res **19:**4413–4419. http://dx.doi.org/10.1093/nar/19.16.4413.
74. **Osuna R, Boylan SA, Bender RA.** 1991. *In vitro* transcription of the histidine utilization (*hutUH*) operon from *Klebsiella aerogenes*. J Bacteriol **173:**116–123.
75. **Abbott ZD, Yakhnin H, Babitzke P, Swanson MS.** 2015. *csrR*, a paralog and direct target of CsrA, promotes *Legionella pneumophila* resilience in water. mBio **6:**e00595. http://dx.doi.org/10.1128/mBio.00595-15.
76. **Lenz DH, Miller MB, Zhu J, Kulkarni RV, Bassler BL.** 2005. CsrA and three redundant small RNAs regulate quorum sensing in *Vibrio cholerae*. Mol Microbiol **58:**1186–1202. http://dx.doi.org/10.1111/j.1365-2958.2005.04902.x.
77. **Heroven AK, Sest M, Pisano F, Scheb-Wetzel M, Steinmann R, Bohme K, Klein J, Munch R, Schomburg D, Dersch P.** 2012. CRP induces switching of the CsrB and CsrC RNAs in *Yersinia pseudotuberculosis* and links nutritional status to virulence. Front Cell Infect Microbiol **2:**158. http://dx.doi.org/10.3389/fcimb.2012.00158.
78. **Nuss AM, Schuster F, Heroven AK, Heine W, Pisano F, Dersch P.** 2014. A direct link between the global regulator PhoP and the Csr regulon in *Yersinia pseudotuberculosis* through the small regulatory RNA CsrC. RNA Biol **11:**580–593. http://dx.doi.org/10.4161/rna.28676.
79. **Teplitski M, Goodier RI, Ahmer BMM.** 2006. Catabolite repression of the SirA regulatory cascade in *Salmonella enterica*. Int J Med Microbiol **296:**449–466. http://dx.doi.org/10.1016/j.ijmm.2006.06.001.
80. **Holmqvist E, Wright PR, Li L, Bischler T, Barquist L, Reinhardt R, Backofen R, Vogel J.** 2016. Global RNA recognition patterns of post-transcriptional regulators Hfq and CsrA revealed by UV crosslinking in vivo. EMBO J **35:**991–1011. http://dx.doi.org/10.15252/embj.201593360.